iScience

CellPress
OPEN ACCESS

Article

A single-cell atlas of human teeth

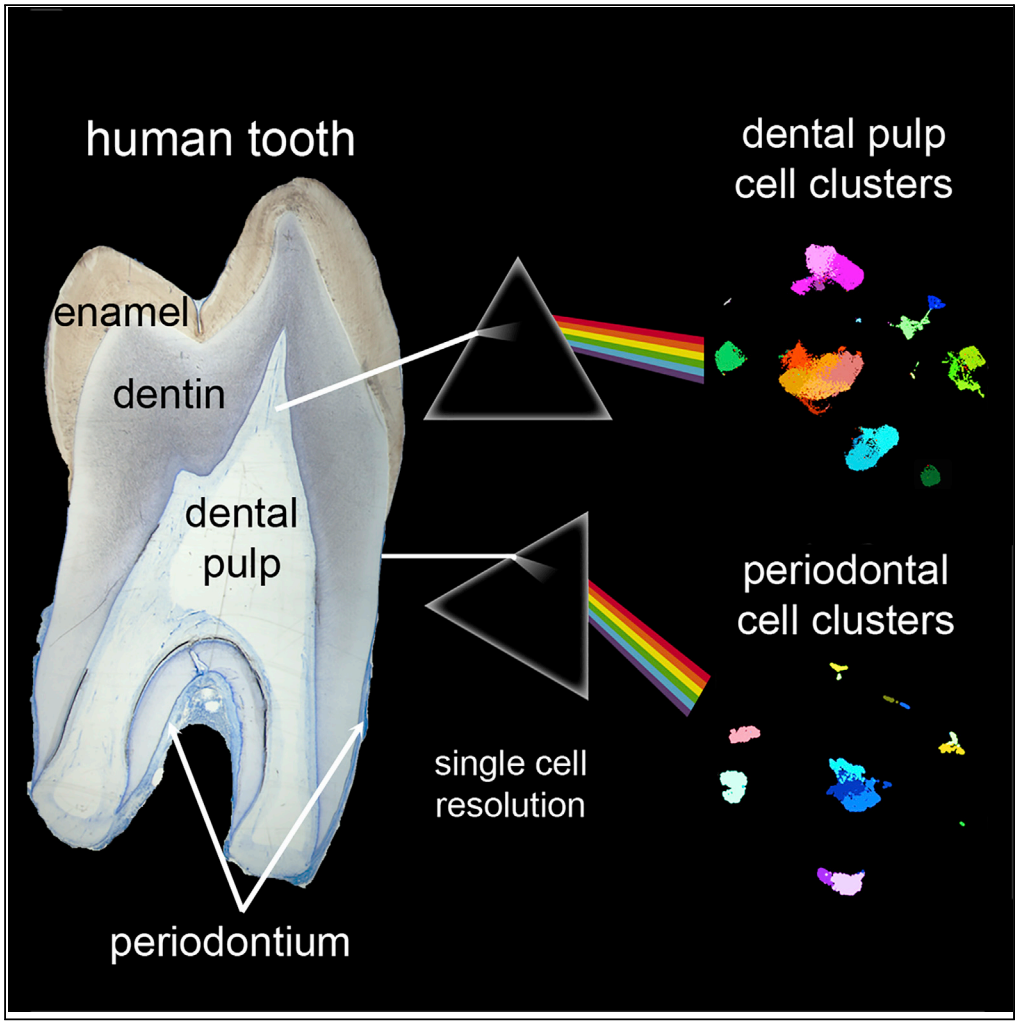

Pierfrancesco Pagella, Laura de Vargas Roditi, Bernd Stadlinger, Andreas E. Moor, Thimios A. Mitsiadis

andreas.moor@bsse.ethz.ch (A.E.M.)
thimios.mitsiadis@zzm.uzh.ch (T.A.M.)

Highlights

Dental atlas of the pulp and periodontal tissues of human teeth

Identification of three common MSC subclusters between dental pulp and periodontium

Dental pulp and periodontal MSCs are similar, and their niches diverge

Pagella et al., iScience *24*, 102405
May 21, 2021
https://doi.org/10.1016/j.isci.2021.102405

iScience

CellPress
OPEN ACCESS

Article

A single-cell atlas of human teeth

Pierfrancesco Pagella,[1,5] Laura de Vargas Roditi,[2,4,5] Bernd Stadlinger,[3] Andreas E. Moor,[2,4,*] and Thimios A. Mitsiadis[1,6,*]

SUMMARY

Teeth exert fundamental functions related to mastication and speech. Despite their great biomedical importance, an overall picture of their cellular and molecular composition is still missing. In this study, we have mapped the transcriptional landscape of the various cell populations that compose human teeth at single-cell resolution, and we analyzed in deeper detail their stem cell populations and their microenvironment. Our study identified great cellular heterogeneity in the dental pulp and the periodontium. Unexpectedly, we found that the molecular signatures of the stem cell populations were very similar, while their respective microenvironments strongly diverged. Our findings suggest that the microenvironmental specificity is a potential source for functional differences between highly similar stem cells located in the various tooth compartments and open new perspectives toward cell-based dental therapeutic approaches.

INTRODUCTION

Teeth are composed of a unique combination of hard and soft tissues. Enamel, the hardest tissue of the human body, covers the crown of the tooth, and it is supported by a second less mineralized tissue, the dentin. The central portion of the tooth is occupied by the dental pulp, a highly vascularized and innervated tissue that is lined by odontoblasts, the cells responsible for dentin formation. The tooth is anchored to the surrounding alveolar bone via the periodontium, which absorbs the various shocks associated with mastication and provides tooth stability by continuously remodeling its extracellular matrix, the periodontal ligament (Nanci, 2013). The development of the tooth results from sequential and reciprocal interactions between cells of the oral epithelium and the cranial neural crest-derived mesenchyme (Kollar, 1986; Mitsiadis and Graf, 2009; Nanci, 2013). Oral epithelial cells give rise to ameloblasts that produce enamel. Dental mesenchymal cells give rise to odontoblasts that form the dentin, as well as to the dental pulp (Mitsiadis and Graf, 2009; Nanci, 2013). Dental pulp and periodontal tissues contain mesenchymal stem cells (MSCs), namely the dental pulp stem cells (DPSCs) and periodontal stem cells (PDSCs) (Gronthos et al., 2000; Roguljic et al., 2013). The epithelial cell remnants in the periodontal space upon dental root completion form an additional tooth-specific epithelial stem cell population (Athanassiou-Papaefthymiou et al., 2015). DPSCs and PDSCs are multipotent and respond to a plethora of cellular, chemical, and physical stimuli to guarantee homeostasis and regeneration of dental tissues. Isolated DPSCs and PDSCs are the subject of intense investigation as possible tools for the regeneration of both dental and non-dental tissues (Chen et al., 2020; Iohara et al., 2011; Lei et al., 2014; Orsini et al., 2018; Ouchi and Nakagawa, 2020; Trubiani et al., 2019; Xuan et al., 2018). *In vivo* studies aiming at the regeneration of dental pulp and periodontal tissues were however not completely successful (Chen et al., 2020; Xu et al., 2019; Xuan et al., 2018). Indeed, the behavior of these and other stem cell populations is regulated by molecular cues produced in their microenvironment by stromal cells, neurons, vascular-related cells, and immune cells, as well as by physical factors such as stiffness, topography, and shear stress (Chacon-Martinez et al., 2018; Machado et al., 2016; Oh and Nor, 2015; Oh et al., 2020; Pagella et al., 2015; Rafii et al., 2016; Scadden, 2014; Yang et al., 2017). Much effort has been spent in the last decades to understand the fine composition of tissues and the cellular and molecular mechanisms that mediate the cross talk between stem cells and their environment to drive regenerative processes (Blache et al., 2018; Chakrabarti et al., 2018; Lane et al., 2014; Mitsiadis et al., 2017a; Oh et al., 2020; Rafii et al., 2016). Concerning teeth, one recent article reported the single-cell RNA sequencing analysis of mouse dental tissue and the human dental pulp, focusing mostly on the continuously growing mouse incisor and on the conservation between species of cellular populations and features that underlie tooth growth (Krivanek et al., 2020). A second single-cell RNA sequencing analysis study in the continuously erupting mouse incisor identified dental epithelial stem cells subpopulations that are important upon tooth injury and contribute to enamel regeneration (Sharir et al., 2019). Despite the great

[1]Orofacial Development and Regeneration, Faculty of Medicine, Institute of Oral Biology, Center of Dental Medicine, University of Zurich, Plattenstrasse 11, 8032 Zurich, Switzerland

[2]Institute of Molecular Cancer Research, University of Zurich, Zurich, Switzerland

[3]Clinic of Cranio-Maxillofacial and Oral Surgery, University of Zurich, Zurich, Switzerland

[4]Present address: Department of Biosystems Science and Engineering, ETH Zürich, Mattenstrasse 26, 4058 Basel, Switzerland

[5]These authors contributed equally

[6]Lead contact

*Correspondence: andreas.moor@bsse.ethz.ch (A.E.M.), thimios.mitsiadis@zzm.uzh.ch (T.A.M.)

https://doi.org/10.1016/j.isci.2021.102405

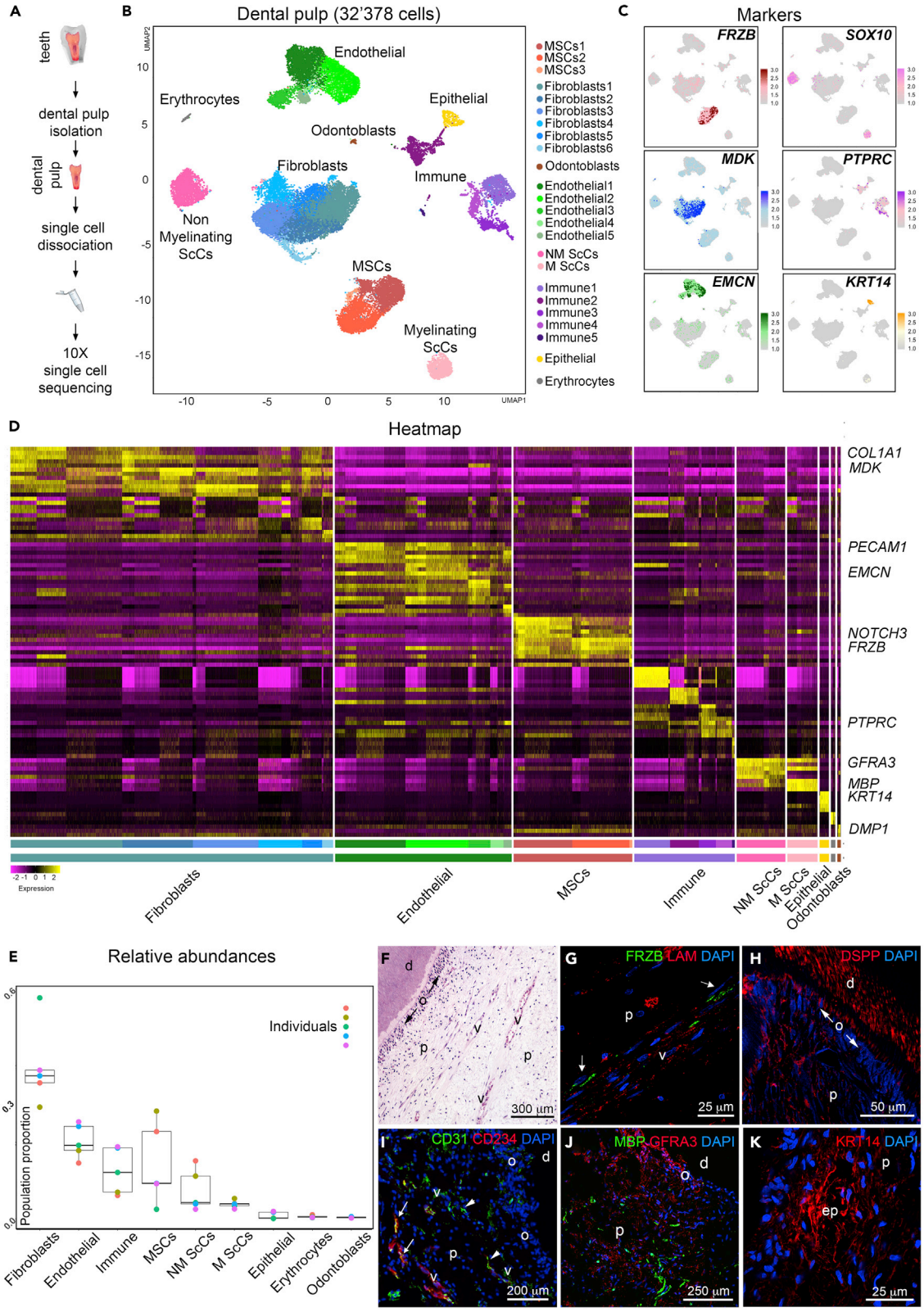
A
teeth
dental pulp isolation
dental pulp
single cell dissociation
10X single cell sequencing
B
Dental pulp (32'378 cells)
Endothelial
Erythrocytes
Epithelial
Odontoblasts
Fibroblasts
Immune
Non Myelinating ScCs
MSCs
Myelinating ScCs
MSCs1
MSCs2
MSCs3
Fibroblasts1
Fibroblasts2
Fibroblasts3
Fibroblasts4
Fibroblasts5
Fibroblasts6
Odontoblasts
Endothelial1
Endothelial2
Endothelial3
Endothelial4
Endothelial5
NM ScCs
M ScCs
Immune1
Immune2
Immune3
Immune4
Immune5
Epithelial
Erythrocytes
C
Markers
FRZB
SOX10
MDK
PTPRC
EMCN
KRT14
D
Heatmap
COL1A1
MDK
PECAM1
EMCN
NOTCH3
FRZB
PTPRC
GFRA3
MBP
KRT14
DMP1
Expression
Fibroblasts
Endothelial
MSCs
Immune
NM ScCs
M ScCs
Epithelial
Odontoblasts
E
Relative abundances
Individuals
Population proportion
F
G
FRZB LAM DAPI
H
DSPP DAPI
I
CD31 CD234 DAPI
J
MBP GFRA3 DAPI
K
KRT14 DAPI
300 µm
25 µm
50 µm
200 µm
250 µm
25 µm

Figure 1. Single-cell RNA sequencing analysis of adult healthy human dental pulps

(A) Schematic representation of the experimental setup.

(B) UMAP visualization of color-coded clustering of the dental pulp (n > 32'000 cells).

(C) Expression of example key genes used for the annotation and the characterization of the clusters.

(D) Heatmap showing expression of most differentially expressed genes between each cluster and all others.

(E) Boxplot of relative abundance of main cell types composing the dental pulp from each patient. Boxes illustrate the interquartile range (25th to 75th percentile), the median is shown as the middle band, and the whiskers extend to 1.5 times the interquartile range from the top (or bottom) of the box to the furthest datum within that distance. Any data points beyond that distance are considered outliers.

(F) Hematoxylin-eosin staining showing the structure of the dental pulp.

(G) Immunofluorescent staining showing localization of FRZB-expressing (green color, white arrows) MSCs around blood vessels (laminin positive, red color).

(H) Immunofluorescent staining showing localization of DSPP-expressing odontoblasts.

(I) Immunofluorescent staining showing CD234-expressing (red color) endothelial cells ($CD31^+$, green color). $CD31^+CD234^+$ cells are marked by arrows; $CD31^+CD234^-$ cells are marked by arrowheads.

(J) Immunofluorescent staining showing localization of MBP-expressing, myelinating Schwann cells (green color), and GFRA3-expressing, non-myelinating Schwann cells (M, red color).

(K) Immunofluorescent staining showing localization of KRT14-expressing epithelial cells (red color). Blue color: DAPI. d, dentin; nf, nerve fibers; o, odontoblasts; p, pulp; v, vessels. Scale bars: (F), 300 μm; (G) and (K), 25 μm; (H), 50 μm; (I), 200 μm; (J), 250 μm.

clinical relevance, the cellular composition of the two main human dental tissues, the dental pulp and the periodontium, has not been investigated in deeper detail.

RESULTS

We used single-cell profiling to elucidate the cellular and molecular composition of human teeth and shed light on fundamental biological questions concerning dental stem cell behavior. We first characterized the cell populations that form the dental pulp and periodontal tissues in human teeth, and thus, we focused on the MSC populations.

Single-cell RNA sequencing analysis of the dental pulp of human teeth

We first analyzed the cellular and molecular composition of the dental pulp of human teeth. For this purpose, we isolated dental pulps from five extracted third molars, dissociated them into single-cell suspensions and proceeded with droplet-based encapsulation (using the 10x Genomics Chromium System) and sequencing. Our analyses yielded a total of 32'378 dental pulp cells (Figure S1). We identified 15 clusters of cells using the graph clustering approach implemented in Seurat v3 (Hafemeister and Satija, 2019) and visualized them using uniform manifold approximation and projection (McInnes et al., 2018) (Figures 1A–1D). Our analysis identified a variety of cell populations including MSCs, fibroblasts, odontoblasts, endothelial cells (ECs), Schwann cells (ScCs), immune cells, epithelial-like cells, and erythrocytes (Figure 1B). MSCs were characterized by the higher expression of *FRZB*, *NOTCH3*, *THY1*, and *MYH11* (Figures 1C, 1D, and 1G) (log-fold change of 2.07, 1.24, 1.54, and 1.4, respectively, and adjusted p value < 0.001, compared to other cell types in the pulp) and represented on average 12% of the dental pulp tissue (mean proportion = 0.12 and standard deviation (sd) = 0.05; Figure 1E). MSCs were localized around the vessels (Figure 1G), where the perivascular niches are formed (Lovschall et al., 2007; Shi and Gronthos, 2003), as well as in the sub-odontoblastic area, which is another potential stem cell niche location in the dental pulp (Mitsiadis and Rahiotis, 2004; Mitsiadis et al., 2003). The fibroblastic compartment composed the bulk of the dental pulp tissue (mean proportion = 0.38 and sd = 0.1; Figure 1E). Different fibroblastic clusters could be identified. Fibroblasts were characterized by the expression of collagen-coding genes (e.g., *COL1A1*; logFC = 0.91 and adjusted p value <0.001) and *MDK* (logFC = 1.44 and adjusted p value <0.001), a gene whose expression is restricted to the dental mesenchyme during mouse odontogenesis (Mitsiadis et al., 1995), as well as by the reduced expression of *FRZB* (logFC = −0.76 and adjusted p value <0.001; Figures 1B–1D). One cluster, characterized by the high expression of osteomodulin/osteoadherin (Figure S3), represented an intermediate state between MSCs and fibroblasts, with shared gene expression from these two groups. Odontoblasts were characterized by the expression of *dentin sialophosphoprotein* (*DSPP*) (Figure 1I) and *dentin matrix acidic phosphoprotein 1* (*DMP1*), genes encoding for phosphoproteins that constitute essential components of the dentin matrix (D'Souza et al., 1997; Liang et al., 2019). ECs, which constitute important components of the MSC microenvironment (Rafii et al., 2016), showed a significant degree of heterogeneity (Figures 1B and 1I, and S4). Three well-defined clusters of ECs were detected. A first cluster was characterized by the expression of *EDN1/CLDN5* and represented arterial ECs (Figure S4). A second endothelial cluster was characterized by the expression of *ACKR1/CD234* (Figures 1I and S4) and represented postcapillary and collecting venules. The third main endothelial cluster was

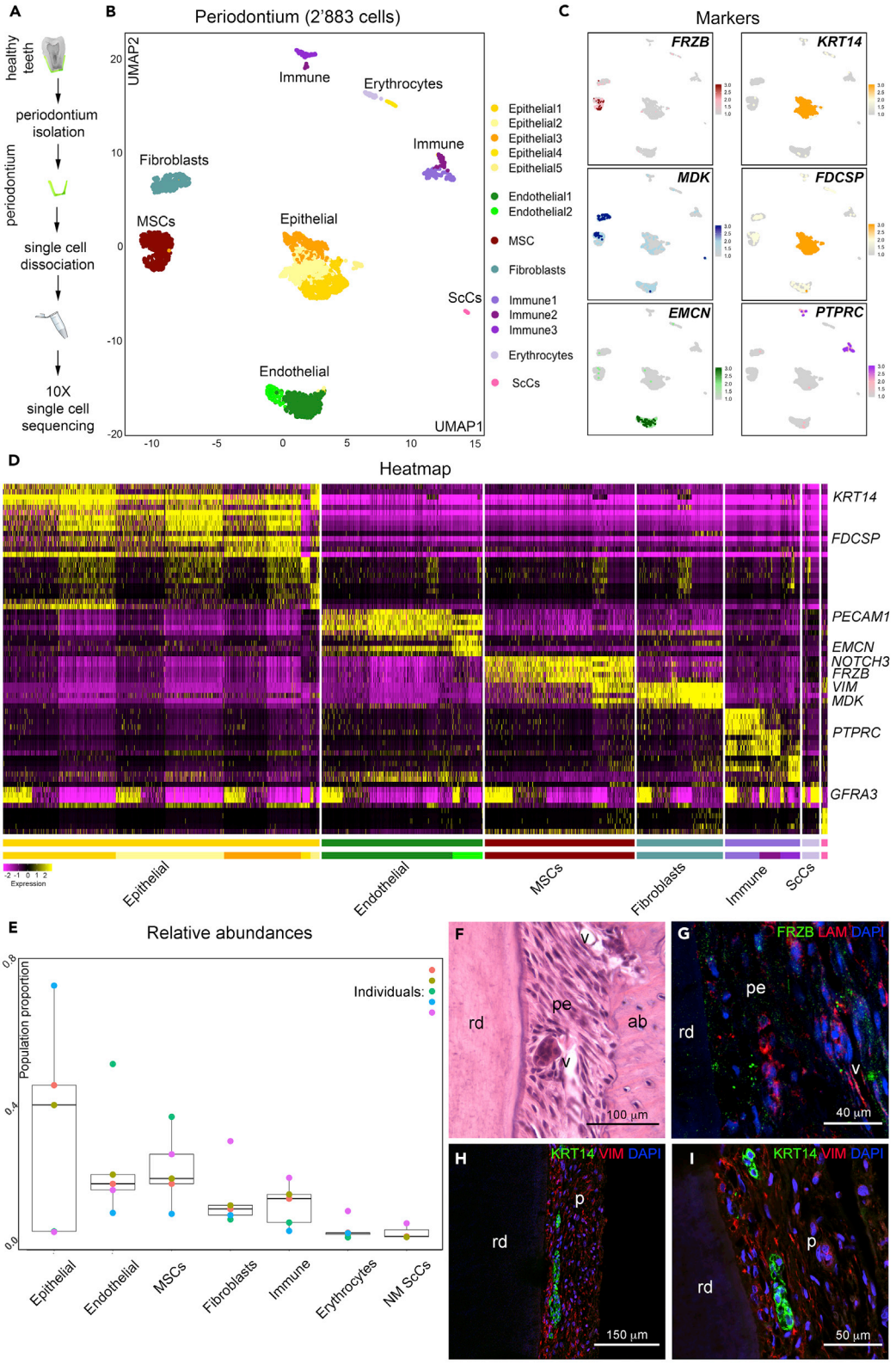
A
healthy teeth
periodontium isolation
periodontium
single cell dissociation
10X single cell sequencing
B
Periodontium (2'883 cells)
UMAP2
UMAP1
Immune
Erythrocytes
Immune
Fibroblasts
MSCs
Epithelial
ScCs
Endothelial
Epithelial1
Epithelial2
Epithelial3
Epithelial4
Epithelial5
Endothelial1
Endothelial2
MSC
Fibroblasts
Immune1
Immune2
Immune3
Erythrocytes
ScCs
C
Markers
FRZB
KRT14
MDK
FDCSP
EMCN
PTPRC
D
Heatmap
KRT14
FDCSP
PECAM1
EMCN
NOTCH3
FRZB
VIM
MDK
PTPRC
GFRA3
Expression
Epithelial
Endothelial
MSCs
Fibroblasts
Immune
ScCs
E
Relative abundances
Population proportion
Individuals:
Epithelial
Endothelial
MSCs
Fibroblasts
Immune
Erythrocytes
NM ScCs
F
v
pe
rd
ab
v
100 µm
G
FRZB LAM DAPI
pe
rd
v
40 µm
H
KRT14 VIM DAPI
p
rd
150 µm
I
KRT14 VIM DAPI
p
rd
50 µm

Figure 2. Single-cell RNA sequencing analysis of the periodontium

(A) Schematic representation of the experimental setup.

(B) UMAP visualization of color-coded clustering of the periodontium (n > 2.800 cells).

(C) Expression of example key genes used for the annotation and the characterization of the clusters.

(D) Heatmap showing expression of the gene most differentially expressed between each cluster and all other ones.

(E) Boxplot of relative abundance of main cell types composing the dental periodontium from each patient. Boxes illustrate the interquartile range (25th to 75th percentile), the median is shown as the middle band, and the whiskers extend to 1.5 times the interquartile range from the top (or bottom) of the box to the furthest datum within that distance. Any data points beyond that distance are considered outliers.

(F) Hematoxylin-eosin staining showing the structure of the periodontium.

(G) Immunofluorescent staining showing localization of *FRZB*-expressing MSCs (green color). Red color: laminin, marking blood vessels; blue color: DAPI.

(H) Immunofluorescent staining showing localization of KRT14-expressing epithelial cells (green color) and vimentin-expressing (VIM) mesenchymal cells (red color) along the periodontium. Blue color: DAPI.

(I) Higher magnification of (H). ab, alveolar bone; lam, laminin; pe, periodontium; rd, root dentin; v, vessel. Scale bars: (F), 100 μm; (G), 40 μm; (I), 50 μm; (H), 150 μm.

characterized by the expression of the *insulin receptor* (*INSR*) and *RGCC* (Figure S4). Immune cells are part of all healthy tissues and organs (Senovilla et al., 2013) and were also consistently detected in the healthy dental pulp tissues. This cluster mostly consisted of T cells and macrophages, characterized by the expression of *PTPRC*, *CD3E*, and *CSF1R* (Figures 1B and S5). Nerve fibers are crucial elements of stem cell niches, as they regulate MSC functions and fates (Pagella et al., 2015). ScCs formed two clearly distinct clusters of $SOX10^+$ cells, identified as myelinating MBP^+-ScCs and non-myelinating $GFRA3^+$-ScCs (Figures 1B, 1C, 1J and S6A). MBP^+-ScCs were mostly localized around major nerve fibers entering the dental pulp, while $GFRA3^+$-ScCs were detected at a distance from nerve fibers and mostly within the sub-odontoblastic regions (Figure 1J), where *NOTCH3*-expressing MSCs were localized. We further identified an epithelial-like cell population within the human dental pulp tissue (Figures 1B and 1C), in accordance with previous reports in human deciduous teeth (Nam and Lee, 2009). These epithelial cells express keratin-coding genes such as *KRT14* and *KRT5*, as well as *stratifin* (*SFN*) (Figures 1C and S6B). We validated the presence of the epithelial cluster within the dental pulp with an immunofluorescent staining against keratin14 (Figure 1K). We finally identified a population of erythrocytes that is characterized by the presence of the *beta*-hemoglobin-coding transcript *HBB*.

Single-cell RNA sequencing analysis of the periodontium of human teeth

We then set out to identify and characterize the cell populations that compose the periodontium of human teeth. We obtained the periodontal tissue by scraping the surface of the apical two-thirds of the roots of five extracted third molars. We dissociated the isolated periodontal tissue to single-cell suspensions and processed them for single-cell RNA sequencing (Figure 2A). We obtained a total of 2'883 periodontal cells (Figure S2A) and identified 15 clusters of cells (Figure 2B). MSCs, fibroblasts, ECs, ScCs, immune cells, epithelial-like, cells and erythrocytes composed the human periodontal tissue (Figure 2B). Similar to the dental pulp tissue, MSCs represented a large fraction of the periodontium (mean proportion = 0.19, sd = 0.11 and se = 0.05). We detected a cluster of MSCs expressing *FRZB*, *NOTCH3*, *MYH11*, and *THY1* (logFC of 1.83, 1.24, 1.47, and 1.61, respectively, and adjusted p value <0.001, compared to other cells in the periodontium; Figures 2B and 2C). The fibroblastic compartment was defined by cells expressing *MDK* (logFC = 1.25 and adjusted p value < 0.001; Figure 2C) and collagen-coding genes such as *COL1A1* (Figures 2B and 2C; logFC = 3.42 and adjusted p value < 0.001). This cluster represented a small fraction of the periodontium (mean proportion = 0.11, sd = 0.08 and se = 0.03; supplemental information Appendix, Figure S2). ECs were more abundant than fibroblasts and represented a big proportion of the periodontal tissues (mean proportion = 0.19, sd = 0.17 and se = 0.07; Figure S2B). We distinguished two main separate ECs clusters, which were characterized by the expression of *EDN1/CLDN5/CXCL12* and *ACKR1/CD234* (Figure 2B), similar to what observed in the dental pulp (Figure 1B). A cluster of *INSR/RGCC*-expressing ECs was observed as an intermediate state between the *EDN1/CLDN5/CXCL1* and *ACKR1/CD234* ECs clusters. ScCs represented a minor population within the periodontium. ScCs expressed *SOX10*, *GFRA3*, *NGF*, and *NGFR* (Figures 2B and 2C; Dataset). The periodontium was characterized by the presence of $PTPRC^+$ immune cells, including T cells ($CD3E^+/CD3D^+$), B cells ($MZB1^+$), monocytes, and macrophages ($CSF1R^+$) (Figure 2C; Dataset). Unexpectedly, we found that the most abundant population of the periodontium consisted of epithelial cells (mean proportion = 0.28, sd = 0.27 and se = 0.12) (Figures 2B–2E and S2B). Epithelial cells formed different subclusters, characterized by the expression of epithelial genes such as *KRT14* and *ODAM*, signaling molecules such as *WNT10A*, and specific sets of interleukin-coding genes such as *IL1A* and *IL1B* (Figure S7). Using immunofluorescent staining, we showed

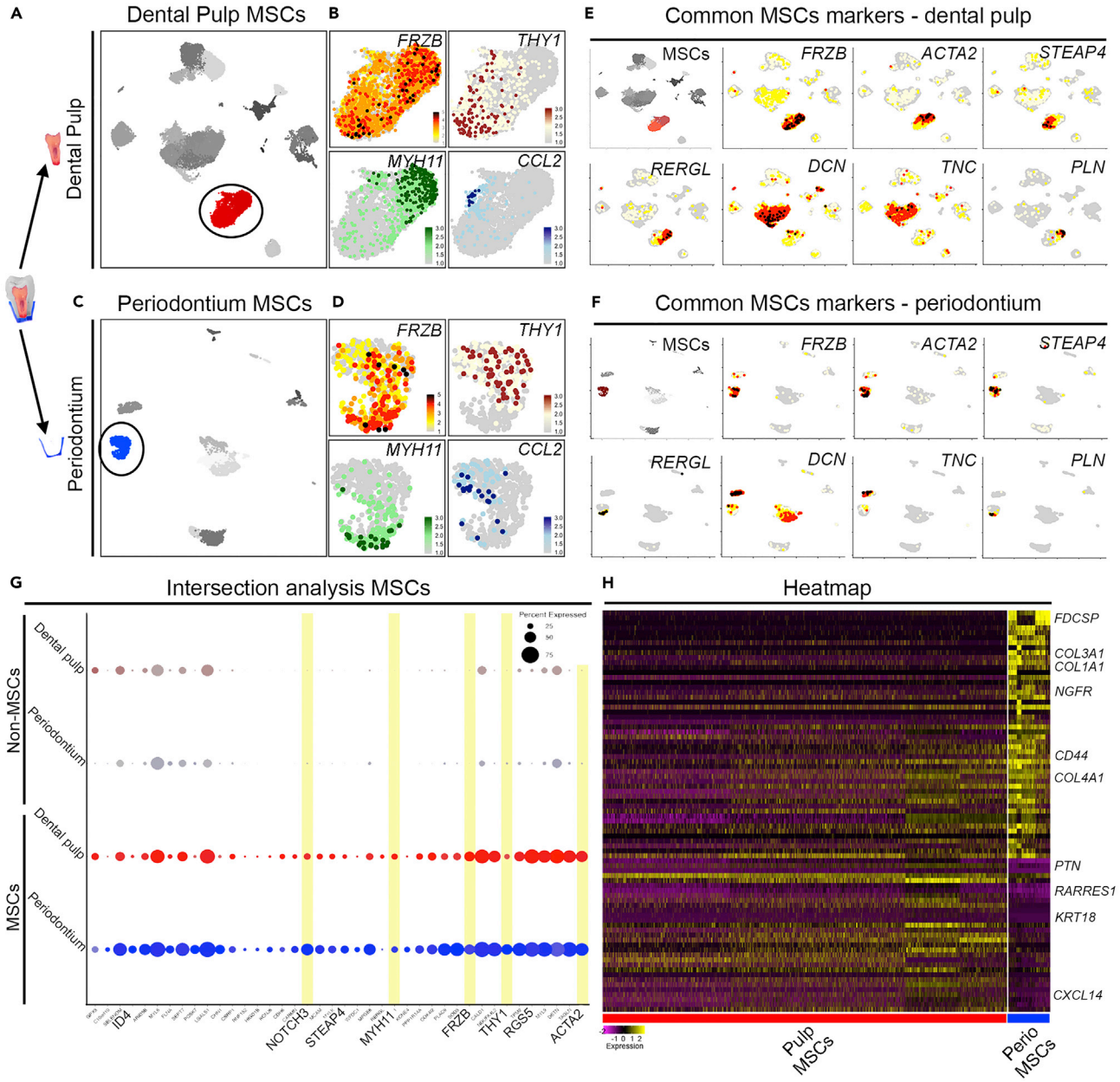

Figure 3. Comparative analysis of the MSC compartment in the pulp and the periodontium

(A) UMAP visualization of pulp clusters, highlighting the MSC compartment.

(B) Feature plots showing genes that characterize the main MSC subclusters within the pulp.

(C) UMAP visualization of periodontium clusters, highlighting the MSC compartment.

(D) Feature plots showing genes that characterize the main MSC subclusters within the periodontium.

(E and F) Feature plots showing the distribution of the expression of common genes characterizing dental pulp (E) and periodontal (F) MSCs. *FRZB* is expressed by all MSCs, both in the dental pulp and in the periodontium. *ACTA2*, *RERGL*, and *PLN* (phospholamban) are particularly enriched in the *MYH11*$^{+}$ MSC subcluster, while *DCN* (decorin) and *STEAP4* are highly expressed in the *THY1*$^{+}$ MSC subcluster. *TNC* (tenascin) is highly expressed in the *CCL2*$^{+}$ MSC subcluster. Previous studies have shown that *TNC* is expressed during odontogenesis in the dental mesenchyme (Vainio et al., 1989) as well as in the mature periodontium at the interface with cementum and with the alveolar bone (Lukinmaa et al., 1991; Midwood et al., 2016).

(G) Dot plot showing the top 40 genes that characterize both dental pulp and periodontal MSCs against other dental cell types. Light yellow highlights genes of particular interest. MSCs in the dental pulp and the periodontium shared the expression of many stem cell markers and genes associated with stem cell function. *MYH11* codes for a myosin heavy chain and its expression has been primarily observed in perivascular smooth muscle cells and pericytes, a common

Figure 3. *Continued*

source of MSCs (Murgai et al., 2017). Similarly, *ACTA2* is often expressed in pericytes. *THY1* codes for CD90, a cell surface protein used as a classical marker for MSCs (An et al., 2018; Balic et al., 2010). *MCAM/CD164* is a classical marker of MSCs in dental and non-dental tissues (Shi and Gronthos, 2003). *RGS5* expression marks the perivascular *NOTCH3*$^+$ MSCs in the dental pulp (Lovschall et al., 2007). Most MSCs populations express *ID4*, which codes for a transcription factor that inhibits cell differentiation (Junankar et al., 2015; Patel et al., 2015).

(H) Heatmap showing differential gene expression between the periodontium and pulp MSCs. See Table S1, for logFC and adjusted p value.

that the epithelial cells are organized in discrete islets along the entire periodontium (Figures 2H and 2I). Finally, we identified a small cluster of erythrocytes expressing *HBB* (Figure 2B).

Comparison of dental pulp and periodontal stem cell populations

The establishment of the single-cell atlas of the dental pulp and periodontium of human teeth allows further analyses and comparisons at the molecular level between these two tissues (Figures 3 and 4). Therefore, we first proceeded with the comparison between the stem cell clusters detected in these two dental components. In both tissues, MSCs were characterized by the expression of *FRZB* and *NOTCH3* (logFC = 2.05 and 1.27 and p values < 0.001; Figures 1C, 1D, 2C, 2D, and 3E–3G). We then analyzed the composition of the dental pulp and periodontal MSC clusters in deeper detail. Upon separate subclustering of the *NOTCH3*$^+$*FRZB*$^+$ pulp and periodontal MSCs, we identified three major MSC subpopulations (Figures 3A–3D). Unexpectedly, the main dental pulp and periodontal MSC populations exhibited very similar molecular signatures. Both compartments contained two main MSC clusters characterized by increased expression of *MYH11* (logFC = 2.00 and p value <0.001) and *THY1* (logFC = 1.63 and p value <0.001), respectively, when compared to all other clusters (Figures 3B and 3D). We detected a second *THY1*-positive (and *MYH11*-negative) MSC cluster, with increased expression of *CCL2* (logFC = 3.46 and p value <0.001 when compared to other clusters; Figures 3B and 3D). The *CCL2*$^+$ MSC cluster also expressed genes associated with the remodeling of the extracellular matrix, such as *TNC* (tenascin C) (Figure 3E).

Next, we merged the dental pulp and periodontium data sets and jointly clustered them to compare the transcriptomes of their MSCs (Figures 3H and 4A). We detected gene expression log-fold changes higher than 0.25 in only 333 genes and as few as 33 genes with a logFC higher than 1 (p values < 0.05, Figure 3H; Table S1). MSCs from the two tissues showed no significant differences in the expression of the already mentioned *NOTCH3*, *FRZB*, *THY1*, and *MYH11*, as well as the other stem cell markers *MCAM/CD146*, *RGS5*, *ACTA2*, and *ID4* (Figure 3G). Some genes were significantly more expressed in periodontal MSCs than in the pulp, such as *CCL2* (logFC = 0.78 and p < 0.001), and those coding for collagens (e.g., *COL3A1*, *COL1A1*, *COL6A1*, *COL6A3*, *COL4A1*) (logFC = 1.65, 1.59, 1.02, 0.70, 0.86, respectively, and adjusted p values < 0.001; Figure 3H; Tables S1 and S3; Figure S8). Periodontal MSCs were also characterized by higher expression of *SPARC/osteonectin*, a secreted molecule fundamental for the regulation of periodontal homeostasis and collagen content (logFC = 1.00 and p value < 0.001; Figure 3H; Tables S1 and S6). In contrast to the periodontal MSCs, dental pulp MSCs expressed higher levels of *CXCL14* and *RARRES1* (logFC = 2.04 and 1.00, respectively, and p values < 0.001; Figure 3H; Table S1). Surprisingly, dental pulp MSCs strongly expressed *KRT18*, a gene previously reported to be exclusively expressed in cells of single-layered and pseudostratified epithelia (logFC = 1.46, p value < 0.001; Table S1, Figure S10).

Comparative analysis of the MSC microenvironment in the dental pulp and periodontium of human teeth

We then compared the two specific MSC niches in the dental pulp and the periodontium (Figures 4 and S2). We observed that their cell compositions diverged in relative proportion for certain cell types, mainly the fibroblastic and epithelial compartments. Fibroblasts represented the most abundant cell population within the dental pulp, while in the periodontium, the proportion of fibroblasts was considerably lower (mean dental pulp = 0.38 and se = 0.04; mean periodontium: 0.11 and se = 0.03. Figures 4B and S2). Likely, due to the high variability of scRNA-seq, it is not possible to statistically confirm this difference using our data set. Genes coding for collagens and matrix metalloproteases (MMPs) were highly expressed by periodontal fibroblasts and MSCs (Figures S8 and S9 and Tables S3 and S5) when compared to their pulp counterparts. Interestingly, genes coding for bone-specific proteins, such as osteonectin (*SPARC*), osteocalcin (*BGLAP*), and bone sialophosphoprotein (*BSP*), were expressed by the periodontal fibroblasts (Figure S11 and Table S6). Periodontal fibroblasts also expressed MGP (matrix Gla protein), a potent inhibitor of mineralization (Figure S11, Table S6). The periodontium was characterized by a larger proportion of cells expressing epithelial cell markers such as *KRT5* and *KRT14* (Figure S2B). As in the case of fibroblasts, it was

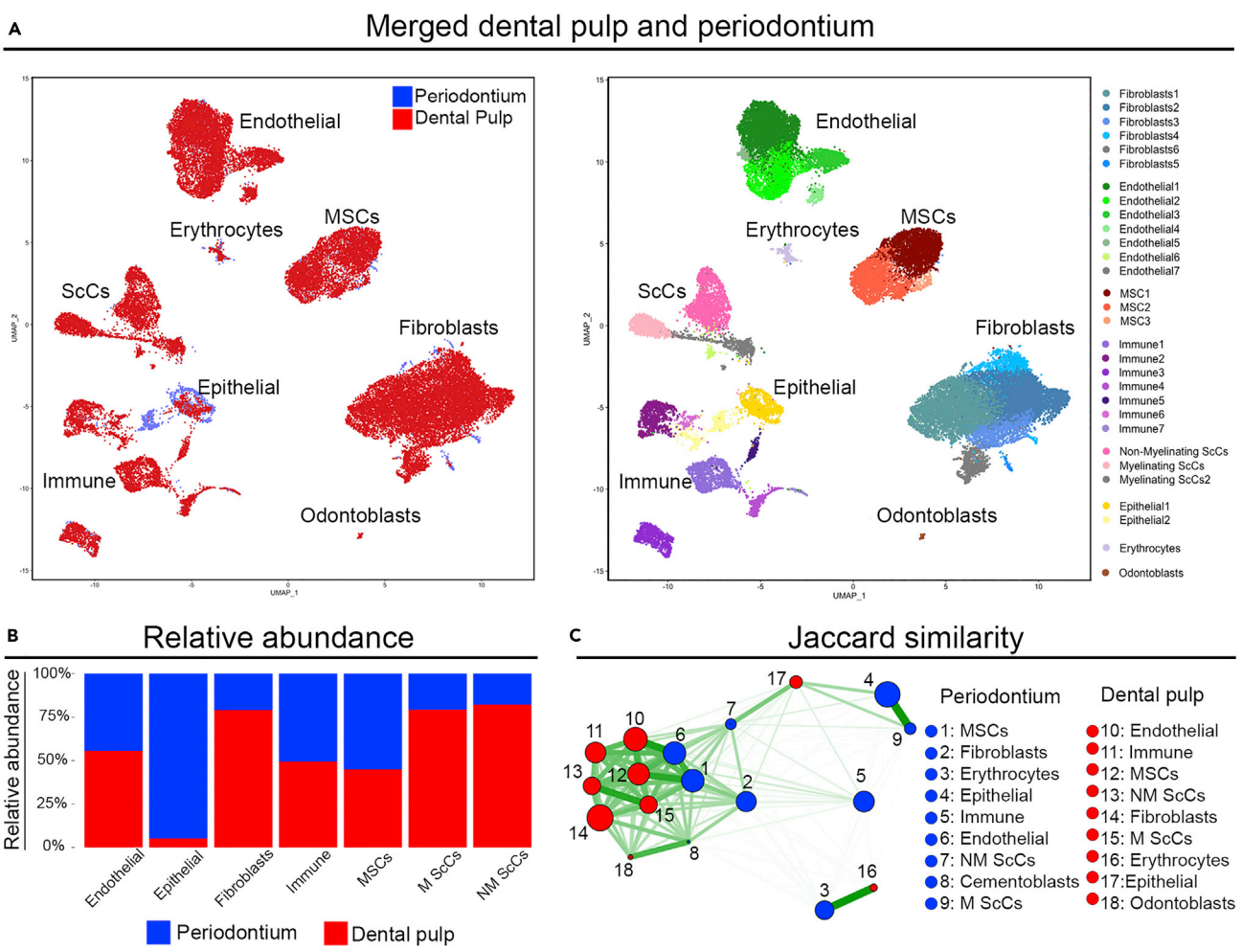

Figure 4. Comparison of the dental pulp and periodontal microenvironment

(A) UMAP plot showing the clusters distribution in the merged dental pulp/periodontium data set.

(B) Comparison of the relative abundance of the different cell types composing the pulp and the periodontium. Epithelial cells are the most abundant cell type in the periodontium, while fibroblasts constitute the most abundant cluster in the dental pulp.

(C) Jaccard similarity plot between the various periodontium and pulp clusters using the top three thousand differentially expressed genes. See supplemental information Appendix, Table S2, for Jaccard similarity ranking.

not possible to statistically confirm this difference in proportion. These periodontal epithelial-like cells expressed different sets of keratin-coding genes when compared to those of the dental pulp (Figure S10, Table S4). In the periodontium, keratin-coding genes such as *Krt14*, *Krt17*, and *Krt19* were not exclusively expressed by epithelial cells but also significantly enriched in fibroblasts and ScCs (Figure S10 and Table S4). The periodontal epithelial-like cells also expressed genes encoding for signaling molecules such as FDCSP (follicular dendritic cell-secreted protein) and WNT10A (Figures 2D and S7). We also found that in the periodontium, the MSCs expressed significantly higher levels of collagen-coding genes (e.g., *COL1A1*, *COL3A1*, *COL6A1*; Figure S8A). We further estimated the pairwise extended Jaccard similarity for all cell types present in the periodontium and dental pulp and ranked these pairwise similarities. This analysis revealed that the three most similar cell types between the periodontium and the dental pulp were, in order, endothelial cells, erythrocytes, and MSCs (Figure 4C and Table S2).

We analyzed the overall dynamics and differentiation trajectories of dental pulp and periodontal MSCs by velocity (Figure S12). We did not identify major differentiation trajectories between different cell types neither in the dental pulp nor in the periodontium. In the dental pulp, endothelial cells showed the most dynamic behavior, while only minor differentiation trajectories were identified within most dental pulp

cell populations (Figure S12). In the periodontium, epithelial-like cells, fibroblasts, and MSCs displayed dynamic behaviors (Figure S12). Periodontal MSCs showed a directional gene expression trajectory from the *MYH11*$^+$ to the *THY1*$^+$ sub-cluster (Figure S12). Periodontal *THY1*$^+$ MSCs co-expressed genes that characterize the fibroblastic compartment, such as the collagen-coding genes, *MMP14*, and *SPARC* (Figures S8 and S11). *MYH11*$^+$ cells might thus constitute the most undifferentiated pool of MSCs within the periodontal tissue, while the *THY1*$^+$ sub-cluster could represent MSCs directed toward the fibroblastic fate.

DISCUSSION

Understanding the fine composition of human organs is of paramount importance to develop regenerative therapies. In particular, unraveling the composition of stem cell populations and their niches is fundamental to drive regenerative processes toward the reconstitution of fully functional tissues and organs. This study revealed that MSCs in the human dental pulp and periodontium are characterized by the expression of *FRZB*, *NOTCH3*, *THY1*, and *MYH11*. *Frzb* has already been shown to mark periodontal ligament cells from very early developmental stages (Mitsiadis et al., 2017b), while its expression in the dental pulp has not yet been reported. Previous studies have also shown that *Notch3* is expressed in perivascular MSCs both in dental and non-dental tissues (Jamal et al., 2015; Lovschall et al., 2007; Wang et al., 2014). Both dental pulp and periodontium MSCs can be subdivided into subpopulations characterized by the expression of the same specific markers *MYH11*, *THY1*, and *CCL2*. *THY1*/*CD90* is a general marker of human mesenchymal stem cells, and it is vastly used to sort human dental pulp stem cells (Dominici et al., 2006; Ledesma-Martinez et al., 2016; Sharpe, 2016). *MYH11* is mostly known to be expressed in smooth muscle cells, and in our data sets, it was generally co-expressed with *ACTA2* (α-smooth muscle actin), recently found to play an important role in MSC cell fate specification (Talele et al., 2015). *CCL2* codes for the chemokine ligand 2, and its expression in MSCs was shown to be a key mediator of their immunomodulatory properties (Giri et al., 2020). Expression of these markers in the dental pulp stem cells is in accordance with the data sets reported in a recent work (Krivanek et al., 2020), while the existence of three distinct MSC subclusters, both in the dental pulp and periodontium, was not reported before. Beyond the expression of these markers, dental MSCs show an overall striking homogeneity, in contrast to current assumptions (Hakki et al., 2015; Lei et al., 2014; Otabe et al., 2012). Indeed, previous studies have shown that although dental pulp and periodontal stem cells possess similar differentiation potentials in generating adipoblasts, myoblasts, chondroblasts, and neurons, their efficacies in forming bone tissues differ (Bai et al., 2010; d'Aquino et al., 2011; Schiraldi et al., 2012; Yagyuu et al., 2010). Human dental pulp and periodontal stem cells do not differ in their specific migratory behavior when cultured separately *in vitro* (Schiraldi et al., 2012). However, when these two cell types are co-cultured, the periodontal MSCs quickly spread and directionally migrate toward the dental pulp stem cells, which exhibit limited proliferative and migratory capabilities (Schiraldi et al., 2012). MSC proliferation and directional migration cues are generally produced by the target tissue, as well as by direct contacts established through the interactions of MSCs with cells composing their niches (Schiraldi et al., 2012; Shellard and Mayor, 2019). The divergent behavior of these MSCs, both in migration and in differentiation, could be due to their interaction with different environments rather than due to intrinsic differences. Our results support that dental MSC homogeneity is counteracted by a great divergence in their niches. In our samples, the dental pulp was composed mostly by fibroblasts, while epithelial cells constituted the most abundant cluster in the periodontium. Fibroblasts and epithelial cells within the dental pulp and the periodontium also expressed very different sets of molecules that could modulate MSC behavior. Genes coding for collagens and MMPs, as well as genes encoding for regulators of mineralization such as osteonectin, were highly expressed by periodontal fibroblasts and MSCs when compared to their dental pulp equivalent. Osteonectin is known to regulate Ca^{2+} deposition during bone formation, but in the periodontium, its function is essential for proper collagen turnover and organization (Luan et al., 2007). Periodontal fibroblasts also expressed MGP, a potent inhibitor of mineralization (Kaipatur et al., 2008). The most abundant periodontal cell type is represented by epithelial-like cells. These periodontal epithelial-like cells expressed genes encoding for signaling molecules such as FDCSP and WNT10A, which exert fundamental roles in the modulation of periodontal MSC proliferation and differentiation (Wei et al., 2011; Xu et al., 2017; Yu et al., 2020). Epithelial cells from the periodontium have been long proposed to constitute a dental epithelial stem cell population, with potential to generate tooth-associated hard tissues such as enamel, dentin, and alveolar bone (Athanassiou-Papaefthymiou et al., 2015; Tsunematsu et al., 2016). We showed that these cells also have signaling properties that could influence the behavior of periodontal MSCs. Overall, the cellular and molecular signature of

the periodontium identified in this study was indicative of its continuous and dynamic remodeling, which is tightly linked to the masticatory function of the teeth, and that requires continuous collagen secretion, extracellular matrix remodeling, and inhibition of mineralization (Takimoto et al., 2015). Taken together, these significant cellular and molecular differences in the microenvironment of the dental pulp and periodontium constitute strong tissue-specific traits. These traits can be indicative of a microenvironment that privileges MSC differentiation toward a fibroblastic-like fate in the periodontium, as opposed to the dental pulp microenvironment, which favors the osteogenic fate of MSCs. Both dental pulp and periodontal MSCs derive from cranial neural crest cell populations, and this common origin provides a developmental basis for the observed similarities in gene expression patterns (Luan et al., 2009). Dental pulp and periodontal precursors display however divergent behaviors from very early developmental stages. Such differences were proposed to be induced from the interaction of similar neural crest cells with different microenvironments (Diekwisch, 2002; Luan et al., 2009; Svandova et al., 2020). These interactions would thus be the basis for the generation of tissues as diverse as the dental pulp, periodontium, and alveolar bone, from common neural crest-derived cell populations (Svandova et al., 2020). Subpopulations of periodontal MSCs indeed maintain for long time a highly migratory behavior, which has been hypothesized to depend as well on the peculiar periodontal microenvironment (Diekwisch, 2002; Luan et al., 2009). Microenvironmental cues would then result in the generation of different mesenchymal cell and stem cell populations via induction of vast epigenetic alterations (Gopinathan et al., 2019; Luan et al., 2009), thus modulating MSC behavior and determining their identity in the dental pulp and periodontium both during development and in adult life.

Two recent articles described the single-cell RNA sequencing analysis of dental tissues (Krivanek et al., 2020; Sharir et al., 2019). One study identified the main cell types that compose the dental pulp and compared their behavior in mice and humans and between human adult and erupting teeth (Krivanek et al., 2020). This work showed that basic features underlying tooth growth, such as lineage hierarchy between *Smoc2*$^{-}$ and *Smoc2*$^{+}$ cells, are conserved between mice and humans (Krivanek et al., 2020). The data sets concerning the human dental pulp presented in this work are in general agreement with our data. Our results provide a significantly more resolved analysis, in which we identified not only the major cell types present within the dental pulp and the periodontium but also their heterogeneity. In a second study, the authors performed single-cell RNA sequencing analysis of the epithelium of the continuously growing mouse incisor and revealed the role of Notch1-expressing stem cells showing that these cells are responsive to tooth injury and contribute to enamel regeneration (Sharir et al., 2019). Overall, these studies are complementary to our work, as they focused mostly on mouse teeth, while they did not investigate in detail the cell types that compose the human dental pulp and periodontium.

Taken together, our findings provide a thorough investigation of the human pulp and periodontal tissues at single-cell resolution, thus representing the basis for future research involving cell-based regenerative treatments.

Limitations of the study

This is the first complete single-cell atlas of human teeth that allows a comparative single-cell RNA analysis of human dental pulp and periodontium. In our data sets, we identified great variability between patients, which was particularly pronounced in the periodontium. The latter could be due to the highly dynamic nature of the periodontium (Luan et al., 2007) and to the peculiar experimental procedure needed to isolate periodontal cells, i.e., scraping them from the surface of the tooth roots. Since our atlas represents cells that survive experimental procedures, the number of odontoblasts in the dental pulp might be underestimated, due to possible damages induced to some of them during the extraction of the dental pulp from the tooth. With our analysis, we observed little differences between dental pulp and periodontal MSCs, which were counteracted by a great divergence in the composition of their niches. We hypothesized that such divergence could be the basis for the observed differences in the behavior of otherwise similar MSCs in the dental pulp and periodontium. This hypothesis requires nevertheless further experimental validation.

Resource availability

Lead contact

Information and requests for resources should be directed to the lead contact, Thimios A. Mitsiadis (thimios.mitsiadis@zzm.uzh.ch).

Materials availability

This study did not generate new unique reagents.

Data and code availability

The accession number for all sequencing data reported in this paper is GEO: GSE161267. All code is publicly available at: https://github.com/TheMoorLab/Tooth.

METHODS

All methods can be found in the accompanying transparent methods supplemental file.

SUPPLEMENTAL INFORMATION

Supplemental information can be found online at https://doi.org/10.1016/j.isci.2021.102405.

ACKNOWLEDGMENTS

We thank Dr. Emilio Yangüez and the Functional Genomics Center Zurich (ETH/University of Zurich) for the processing of the samples for single-cell RNA sequencing. We thank Ms. Kendra Wernlé and Ms. Madeline Fellner (Institute for Oral Biology, University of Zurich) for technical assistance. Imaging was performed with equipment maintained by the Center for Microscopy and Image Analysis, University of Zurich. This work was financially supported by the University of Zurich and by the Swiss National Science Foundation (310030_197782).

AUTHOR CONTRIBUTION

Conceptualization, T.A.M., A.E.M., and P.P.; methodology, T.A.M, A.E.M., P.P., L.d.V.R., and B.S.; data analysis, A.E.M. and L.d.V.R.; validation, T.A.M., A.E.M., L.d.V.R., and P.P.; formal analysis, P.P., L.d.V.R., A.E.M., and T.A.M.; investigation, P.P. and L.d.V.R.; resources, T.A.M. and A.E.M.; data curation, L.d.V.R. and A.E.M.; writing – original draft, P.P. and T.A.M.; writing – review & editing, P.P., L.d.V.R., B.S., A.E.M., and T.A.M.; visualization, P.P., L.d.V.R., A.M., and T.A.M.; supervision, T.A.M. and A.E.M.; project administration, T.A.M. and A.E.M.; funding acquisition, T.A.M.

DECLARATION OF INTERESTS

The authors declare no competing interests.

Received: February 24, 2021
Revised: March 29, 2021
Accepted: April 6, 2021
Published: May 21, 2021

REFERENCES

An, Z., Sabalic, M., Bloomquist, R.F., Fowler, T.E., Streelman, T., and Sharpe, P.T. (2018). A quiescent cell population replenishes mesenchymal stem cells to drive accelerated growth in mouse incisors. Nat. Commun. *9*, 378.

Athanassiou-Papaefthymiou, M., Papagerakis, P., and Papagerakis, S. (2015). Isolation and characterization of human adult epithelial stem cells from the periodontal ligament. J. Dent Res. *94*, 1591–1600.

Bai, Y., Bai, Y., Matsuzaka, K., Hashimoto, S., Kokubu, E., Wang, X., and Inoue, T. (2010). Formation of bone-like tissue by dental follicle cells co-cultured with dental papilla cells. Cell Tissue Res *342*, 221–231.

Balic, A., Aguila, H.L., Caimano, M.J., Francone, V.P., and Mina, M. (2010). Characterization of stem and progenitor cells in the dental pulp of erupted and unerupted murine molars. Bone *46*, 1639–1651.

Blache, U., Vallmajo-Martin, Q., Horton, E.R., Guerrero, J., Djonov, V., Scherberich, A., Erler, J.T., Martin, I., Snedeker, J.G., Milleret, V., et al. (2018). Notch-inducing hydrogels reveal a perivascular switch of mesenchymal stem cell fate. EMBO Rep. *19*, e45964.

Chacon-Martinez, C.A., Koester, J., and Wickstrom, S.A. (2018). Signaling in the stem cell niche: regulating cell fate, function and plasticity. Development *145*, dev165399.

Chakrabarti, R., Celia-Terrassa, T., Kumar, S., Hang, X., Wei, Y., Choudhury, A., Hwang, J., Peng, J., Nixon, B., Grady, J.J., et al. (2018). Notch ligand Dll1 mediates cross-talk between mammary stem cells and the macrophageal niche. Science *360*, eaan4153.

Chen, H., Fu, H., Wu, X., Duan, Y., Zhang, S., Hu, H., Liao, Y., Wang, T., Yang, Y., Chen, G., et al. (2020). Regeneration of pulpo-dentinal-like complex by a group of unique multipotent CD24a(+) stem cells. Sci. Adv. *6*, eaay1514.

d'Aquino, R., Tirino, V., Desiderio, V., Studer, M., De Angelis, G.C., Laino, L., De Rosa, A., Di Nucci, D., Martino, S., Paino, F., et al. (2011). Human neural crest-derived postnatal cells exhibit remarkable embryonic attributes either in vitro or in vivo. Eur. Cell Mater. *21*, 304–316.

D'Souza, R.N., Cavender, A., Sunavala, G., Alvarez, J., Ohshima, T., Kulkarni, A.B., and MacDougall, M. (1997). Gene expression patterns of murine dentin matrix protein 1 (Dmp1) and dentin sialophosphoprotein (DSPP) suggest distinct developmental functions in vivo. J. Bone Miner. Res. *12*, 2040–2049.

Diekwisch, T.G. (2002). Pathways and fate of migratory cells during late tooth organogenesis. Connect. Tissue Res. *43*, 245–256.

Dominici, M., Le Blanc, K., Mueller, I., Slaper-Cortenbach, I., Marini, F., Krause, D., Deans, R., Keating, A., Prockop, D., and Horwitz, E. (2006). Minimal criteria for defining multipotent mesenchymal stromal cells. The International Society for Cellular Therapy position statement. Cytotherapy *8*, 315–317.

Giri, J., Das, R., Nylen, E., Chinnadurai, R., and Galipeau, J. (2020). CCL2 and CXCL12 derived from mesenchymal stromal cells cooperatively polarize IL-10+ tissue macrophages to mitigate gut injury. Cell Rep. *30*, 1923–1934 e1924.

Gopinathan, G., Foyle, D., Luan, X., and Diekwisch, T.G.H. (2019). The Wnt antagonist SFRP1: a key regulator of periodontal mineral homeostasis. Stem Cells Dev. *28*, 1004–1014.

Gronthos, S., Mankani, M., Brahim, J., Robey, P.G., and Shi, S. (2000). Postnatal human dental pulp stem cells (DPSCs) in vitro and in vivo. Proc. Natl. Acad. Sci. U S A *97*, 13625–13630.

Hafemeister, C., and Satija, R. (2019). Normalization and Variance Stabilization of Single-Cell RNA-Seq Data Using Regularized Negative Binomial Regression (bioRxiv), p. 576827.

Hakki, S.S., Kayis, S.A., Hakki, E.E., Bozkurt, S.B., Duruksu, G., Unal, Z.S., Turac, G., and Karaoz, E. (2015). Comparison of mesenchymal stem cells isolated from pulp and periodontal ligament. J. Periodontol. *86*, 283–291.

Iohara, K., Imabayashi, K., Ishizaka, R., Watanabe, A., Nabekura, J., Ito, M., Matsushita, K., Nakamura, H., and Nakashima, M. (2011). Complete pulp regeneration after pulpectomy by transplantation of CD105+ stem cells with stromal cell-derived factor-1. Tissue Eng. A *17*, 1911–1920.

Jamal, M., Chogle, S.M., Karam, S.M., and Huang, G.T. (2015). NOTCH3 is expressed in human apical papilla and in subpopulations of stem cells isolated from the tissue. Genes Dis. *2*, 261–267.

Junankar, S., Baker, L.A., Roden, D.L., Nair, R., Elsworth, B., Gallego-Ortega, D., Lacaze, P., Cazet, A., Nikolic, I., Teo, W.S., et al. (2015). ID4 controls mammary stem cells and marks breast cancers with a stem cell-like phenotype. Nat. Commun. *6*, 6548.

Kaipatur, N.R., Murshed, M., and McKee, M.D. (2008). Matrix Gla protein inhibition of tooth mineralization. J. Dent Res. *87*, 839–844.

Kollar, E.J. (1986). Tissue interactions in development of teeth and related ectodermal derivatives. Dev. Biol. *4*, 297–313.

Krivanek, J., Soldatov, R.A., Kastriti, M.E., Chontorotzea, T., Herdina, A.N., Petersen, J., Szarowska, B., Landova, M., Matejova, V.K., Holla, L.I., et al. (2020). Dental cell type atlas reveals stem and differentiated cell types in mouse and human teeth. Nat. Commun. *11*, 4816.

Lane, S.W., Williams, D.A., and Watt, F.M. (2014). Modulating the stem cell niche for tissue regeneration. Nat. Biotechnol. *32*, 795–803.

Ledesma-Martinez, E., Mendoza-Nunez, V.M., and Santiago-Osorio, E. (2016). Mesenchymal stem cells derived from dental pulp: a Review. Stem Cells Int. *2016*, 4709572.

Lei, M., Li, K., Li, B., Gao, L.N., Chen, F.M., and Jin, Y. (2014). Mesenchymal stem cell characteristics of dental pulp and periodontal ligament stem cells after in vivo transplantation. Biomaterials *35*, 6332–6343.

Liang, T., Zhang, H., Xu, Q., Wang, S., Qin, C., and Lu, Y. (2019). Mutant dentin sialophosphoprotein causes dentinogenesis imperfecta. J. Dent. Res. *98*, 912–919.

Lovschall, H., Mitsiadis, T.A., Poulsen, K., Jensen, K.H., and Kjeldsen, A.L. (2007). Coexpression of Notch3 and Rgs5 in the pericyte-vascular smooth muscle cell axis in response to pulp injury. Int. J. Dev. Biol. *51*, 715–721.

Luan, X., Dangaria, S., Ito, Y., Walker, C.G., Jin, T., Schmidt, M.K., Galang, M.T., and Druzinsky, R. (2009). Neural crest lineage segregation: a blueprint for periodontal regeneration. J. Dent. Res. *88*, 781–791.

Luan, X., Ito, Y., Holliday, S., Walker, C., Daniel, J., Galang, T.M., Fukui, T., Yamane, A., Begole, E., Evans, C., et al. (2007). Extracellular matrix-mediated tissue remodeling following axial movement of teeth. J. Histochem. Cytochem. *55*, 127–140.

Lukinmaa, P.L., Mackie, E.J., and Thesleff, I. (1991). Immunohistochemical localization of the matrix glycoproteins–tenascin and the ED-sequence-containing form of cellular fibronectin–in human permanent teeth and periodontal ligament. J. Dent. Res. *70*, 19–26.

Machado, C.V., Passos, S.T., Campos, T.M., Bernardi, L., Vilas-Boas, D.S., Nor, J.E., Telles, P.D., and Nascimento, I.L. (2016). The dental pulp stem cell niche based on aldehyde dehydrogenase 1 expression. Int. Endod. J. *49*, 755–763.

McInnes, L., Healy, J., Saul, N., and Grossberger, L. (2018). UMAP: uniform manifold approximation and projection. J. Open Access Softw. *3*, 861.

Midwood, K.S., Chiquet, M., Tucker, R.P., and Orend, G. (2016). Tenascin-C at a glance. J. Cell Sci. *129*, 4321–4327.

Mitsiadis, T.A., Caton, J., Pagella, P., Orsini, G., and Jimenez-Rojo, L. (2017a). Monitoring Notch signaling-associated activation of stem cell niches within injured dental pulp. Front. Physiol. *8*, 372.

Mitsiadis, T.A., and Graf, D. (2009). Cell fate determination during tooth development and regeneration. Birth Defects Res. C Embryo Today *87*, 199–211.

Mitsiadis, T.A., Muramatsu, T., Muramatsu, H., and Thesleff, I. (1995). Midkine (MK), a heparin-binding growth/differentiation factor, is regulated by retinoic acid and epithelial-mesenchymal interactions in the developing mouse tooth, and affects cell proliferation and morphogenesis. J. Cell Biol. *129*, 267–281.

Mitsiadis, T.A., Pagella, P., and Cantu, C. (2017b). Early determination of the periodontal domain by the Wnt-antagonist Frzb/Sfrp3. Front. Physiol. *8*, 936.

Mitsiadis, T.A., and Rahiotis, C. (2004). Parallels between tooth development and repair: conserved molecular mechanisms following carious and dental injury. J. Dent. Res. *83*, 896–902.

Mitsiadis, T.A., Romeas, A., Lendahl, U., Sharpe, P.T., and Farges, J.C. (2003). Notch2 protein distribution in human teeth under normal and pathological conditions. Exp. Cell Res. *282*, 101–109.

Murgai, M., Ju, W., Eason, M., Kline, J., Beury, D.W., Kaczanowska, S., Miettinen, M.M., Kruhlak, M., Lei, H., Shern, J.F., et al. (2017). KLF4-dependent perivascular cell plasticity mediates pre-metastatic niche formation and metastasis. Nat. Med. *23*, 1176–1190.

Nam, H., and Lee, G. (2009). Identification of novel epithelial stem cell-like cells in human deciduous dental pulp. Biochem. Biophys. Res. Commun. *386*, 135–139.

Nanci, A. (2013). Ten Cate's Oral Histology, 8th edn (Elsevier).

Oh, M., and Nor, J.E. (2015). The perivascular niche and self-renewal of stem cells. Front. Physiol. *6*, 367.

Oh, M., Zhang, Z., Mantesso, A., Oklejas, A.E., and Nor, J.E. (2020). Endothelial-initiated crosstalk regulates dental pulp stem cell self-renewal. J. Dent. Res. *99*, 1102–1111.

Orsini, G., Pagella, P., and Mitsiadis, T.A. (2018). Modern trends in dental medicine: an update for internists. Am. J. Med. *131*, 1425–1430.

Otabe, K., Muneta, T., Kawashima, N., Suda, H., Tsuji, K., and Sekiya, I. (2012). Comparison of gingiva, dental pulp, and periodontal ligament cells from the standpoint of mesenchymal stem cell properties. Cell Med. *4*, 13–21.

Ouchi, T., and Nakagawa, T. (2020). Mesenchymal stem cell-based tissue regeneration therapies for periodontitis. Regen. Ther. *14*, 72–78.

Pagella, P., Neto, E., Lamghari, M., and Mitsiadis, T.A. (2015). Investigation of orofacial stem cell niches and their innervation through microfluidic devices. Eur. Cell. Mater. *29*, 213–223.

Patel, D., Morton, D.J., Carey, J., Havrda, M.C., and Chaudhary, J. (2015). Inhibitor of differentiation 4 (ID4): from development to cancer. Biochim. Biophys. Acta *1855*, 92–103.

Rafii, S., Butler, J.M., and Ding, B.S. (2016). Angiocrine functions of organ-specific endothelial cells. Nature *529*, 316–325.

Roguljic, H., Matthews, B.G., Yang, W., Cvija, H., Mina, M., and Kalajzic, I. (2013). In vivo identification of periodontal progenitor cells. J. Dent. Res. *92*, 709–715.

Scadden, D.T. (2014). Nice neighborhood: emerging concepts of the stem cell niche. Cell *157*, 41–50.

Schiraldi, C., Stellavato, A., D'Agostino, A., Tirino, V., d'Aquino, R., Woloszyk, A., De Rosa, A., Laino, L., Papaccio, G., and Mitsiadis, T.A. (2012).

Fighting for territories: time-lapse analysis of dental pulp and dental follicle stem cells in co-culture reveals specific migratory capabilities. Eur. Cell Mater. *24*, 426–440.

Senovilla, L., Galluzzi, L., Zitvogel, L., and Kroemer, G. (2013). Immunosurveillance as a regulator of tissue homeostasis. Trends Immunol. *34*, 471–481.

Sharir, A., Marangoni, P., Zilionis, R., Wan, M., Wald, T., Hu, J.K., Kawaguchi, K., Castillo-Azofeifa, D., Epstein, L., Harrington, K., et al. (2019). A large pool of actively cycling progenitors orchestrates self-renewal and injury repair of an ectodermal appendage. Nat. Cell Biol. *21*, 1102–1112.

Sharpe, P.T. (2016). Dental mesenchymal stem cells. Development *143*, 2273–2280.

Shellard, A., and Mayor, R. (2019). Integrating chemical and mechanical signals in neural crest cell migration. Curr. Opin. Genet. Dev. *57*, 16–24.

Shi, S., and Gronthos, S. (2003). Perivascular niche of postnatal mesenchymal stem cells in human bone marrow and dental pulp. J. Bone Miner. Res. *18*, 696–704.

Svandova, E., Peterkova, R., Matalova, E., and Lesot, H. (2020). Formation and developmental specification of the odontogenic and osteogenic mesenchymes. Front. Cell Dev. Biol. *8*, 640.

Takimoto, A., Kawatsu, M., Yoshimoto, Y., Kawamoto, T., Seiryu, M., Takano-Yamamoto, T., Hiraki, Y., and Shukunami, C. (2015). Scleraxis and osterix antagonistically regulate tensile force-responsive remodeling of the periodontal ligament and alveolar bone. Development *142*, 787–796.

Talele, N.P., Fradette, J., Davies, J.E., Kapus, A., and Hinz, B. (2015). Expression of alpha-smooth muscle actin determines the fate of mesenchymal stromal cells. Stem Cell Rep. *4*, 1016–1030.

Trubiani, O., Pizzicannella, J., Caputi, S., Marchisio, M., Mazzon, E., Paganelli, R., Paganelli, A., and Diomede, F. (2019). Periodontal ligament stem cells: current knowledge and future perspectives. Stem Cells Dev. *28*, 995–1003.

Tsunematsu, T., Fujiwara, N., Yoshida, M., Takayama, Y., Kujiraoka, S., Qi, G., Kitagawa, M., Kondo, T., Yamada, A., Arakaki, R., et al. (2016). Human odontogenic epithelial cells derived from epithelial rests of Malassez possess stem cell properties. Lab Invest. *96*, 1063–1075.

Vainio, S., Jalkanen, M., and Thesleff, I. (1989). Syndecan and tenascin expression is induced by epithelial-mesenchymal interactions in embryonic tooth mesenchyme. J. Cell Biol. *108*, 1945–1953.

Wang, Y., Pan, L., Moens, C.B., and Appel, B. (2014). Notch3 establishes brain vascular integrity by regulating pericyte number. Development *141*, 307–317.

Wei, N., Yu, H., Yang, S., Yang, X., Yuan, Q., Man, Y., and Gong, P. (2011). Effect of FDC-SP on the phenotype expression of cultured periodontal ligament cells. Arch. Med. Sci. *7*, 235–241.

Xu, M., Horrell, J., Snitow, M., Cui, J., Gochnauer, H., Syrett, C.M., Kallish, S., Seykora, J.T., Liu, F., Gaillard, D., et al. (2017). WNT10A mutation causes ectodermal dysplasia by impairing progenitor cell proliferation and KLF4-mediated differentiation. Nat. Commun. *8*, 15397.

Xu, X.Y., Li, X., Wang, J., He, X.T., Sun, H.H., and Chen, F.M. (2019). Concise Review: periodontal tissue regeneration using stem cells: strategies and translational considerations. Stem Cells Transl. Med. *8*, 392–403.

Xuan, K., Li, B., Guo, H., Sun, W., Kou, X., He, X., Zhang, Y., Sun, J., Liu, A., Liao, L., et al. (2018). Deciduous autologous tooth stem cells regenerate dental pulp after implantation into injured teeth. Sci. Transl Med. *10*, eaaf3227.

Yagyuu, T., Ikeda, E., Ohgushi, H., Tadokoro, M., Hirose, M., Maeda, M., Inagake, K., and Kirita, T. (2010). Hard tissue-forming potential of stem/progenitor cells in human dental follicle and dental papilla. Arch. Oral Biol. *55*, 68–76.

Yang, H., Adam, R.C., Ge, Y., Hua, Z.L., and Fuchs, E. (2017). Epithelial-mesenchymal micro-niches govern stem cell lineage choices. Cell *169*, 483–496.e413.

Yu, M., Liu, Y., Wang, Y., Wong, S.W., Wu, J., Liu, H., Feng, H., and Han, D. (2020). Epithelial Wnt10a is essential for tooth root furcation morphogenesis. J. Dent. Res. *99*, 311–319.

iScience, Volume *24*

Supplemental information

A single-cell atlas of human teeth

Pierfrancesco Pagella, Laura de Vargas Roditi, Bernd Stadlinger, Andreas E. Moor, and Thimios A. Mitsiadis

Supplementary Figures

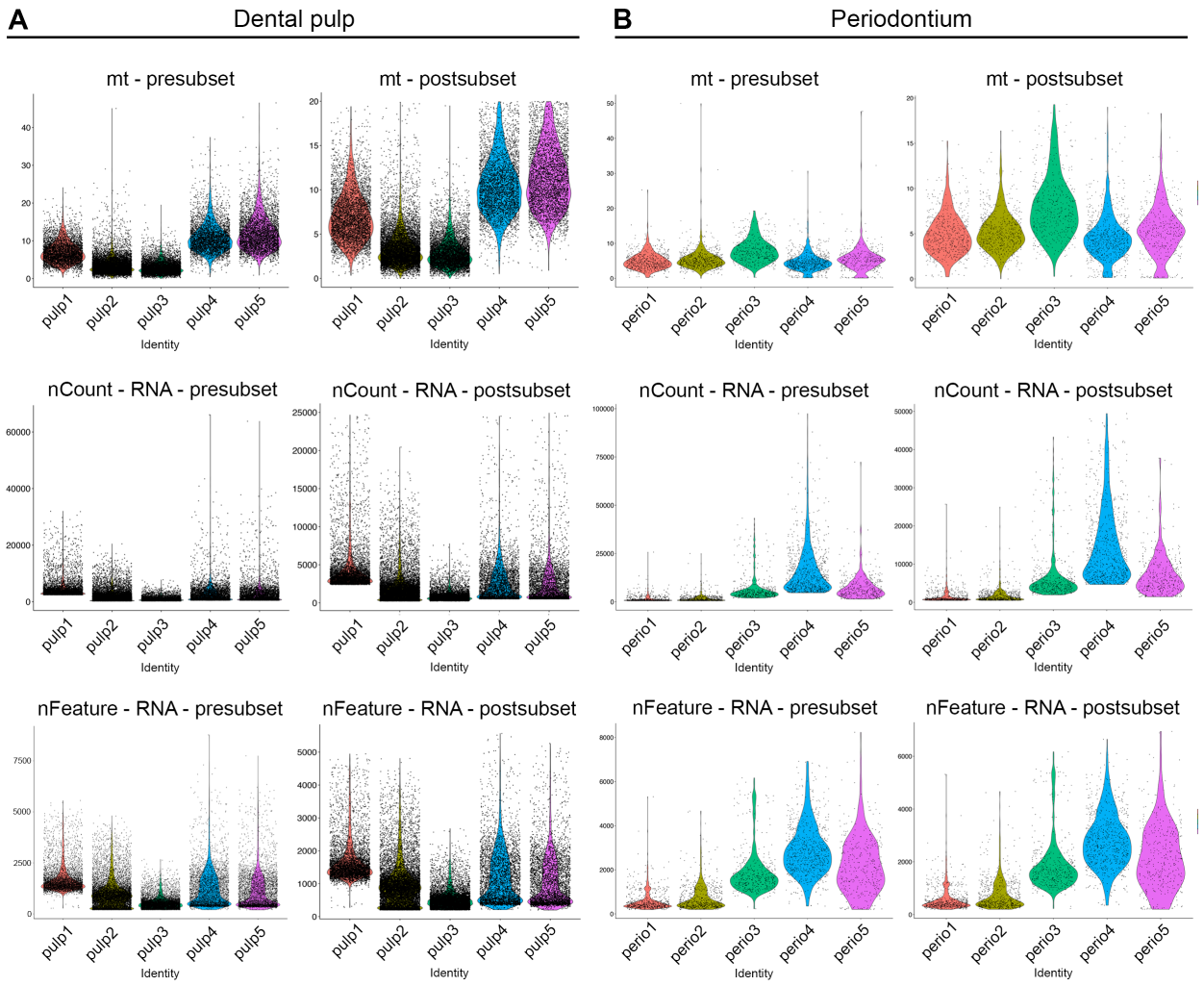

Fig. S1. Quality control and pre-processing of single-cell pulp (A) and periodontium (B) data, related to Figure 1 and Figure 2. Violin plots illustrate distribution of percentage of mitochondrial genes (mt), number of UMI counts (nCount) and number of genes with at least one UMI count (nFeature) per cell prior and after subsetting cells according to the following quality control measures: cells with a percentage of mitochondrial genes above 20 were excluded, as well as cells with less than

200 genes. Healthy pulp and periodontal cells with UMI counts above 25'000 and 50'000, respectively were also excluded.

A Samples details

	Dental pulp	Periodontium
number of samples	5	5
total number of cells	32378	2883
median number of cells per sample	5100	615
mean number of cells per sample	6475.6	576.6
sd number of cells	3022.7	152.9
median genes	830	1333
mean genes	1017.9	1612.5
sd genes	732.7	1255.8

B Relative abundance by cell type

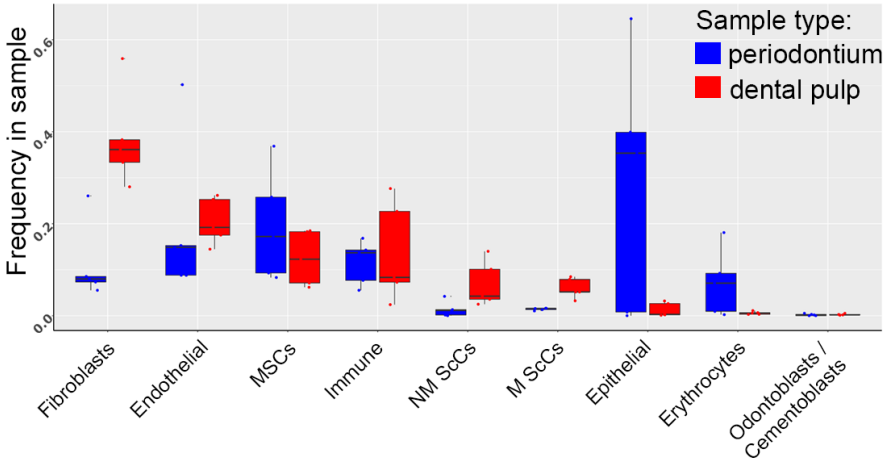

Fig. S2. Quantitative details of dental pulp and periodontal samples, related to Figure 1, Figure 2, Figure 4. A) Sample size and statistics. B) Relative abundance of cell types in the pulp (red) and periodontium (blue); Boxes illustrate the interquartile range (25th to 75th percentile), the median is shown as the middle band, and the whiskers extend to 1.5 times the interquartile range from the top (or bottom) of the box to the furthest datum within that distance. Any data points beyond that distance are considered outliers.

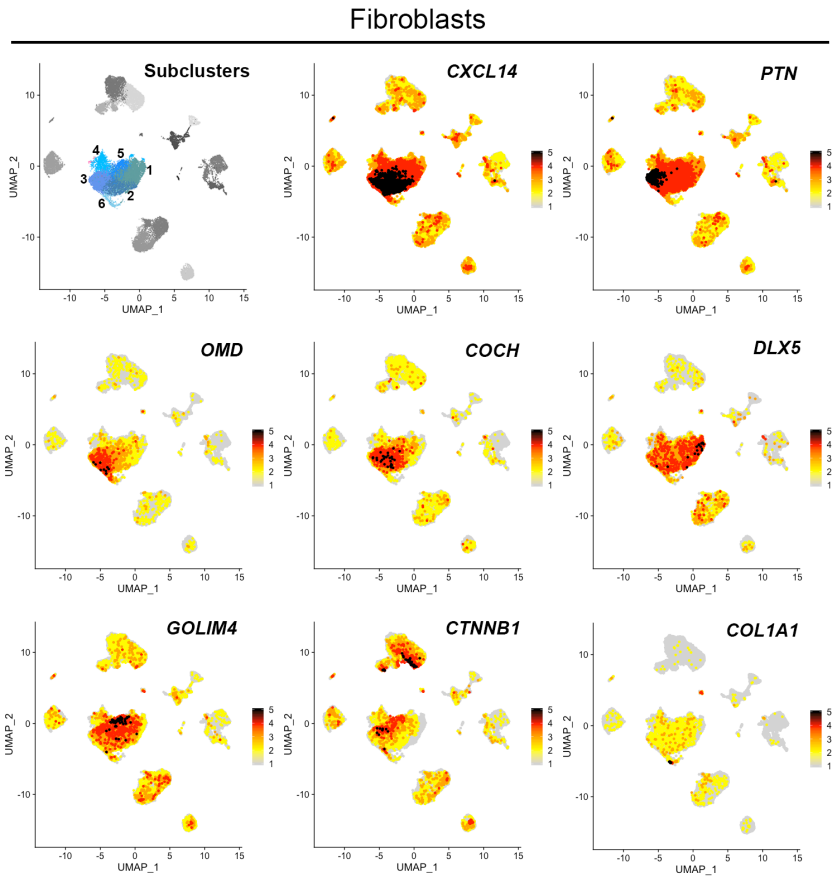

Fig. S3. Feature plots showing the expression of genes characterizing specific subclusters of dental pulp fibroblasts, related to Figure 1. 5 subclusters could be identified within fibroblasts. *CXCL14* was generally expressed by fibroblasts, and it was particularly enriched in subclusters 2 and 3. *CXCL14* expression is associated with angiogenic potential and overall chemoattractant properties (Hayashi et al., 2015). Subcluster 3 showed higher expression of the dental mesenchyme marker *PTN* (pleiotrophin), which is associated with odontoblastic differentiation potential (Mitsiadis et al., 1995). Cluster 6 was characterized by higher expression of *Osteomodulin/Osteoadherin* (*OMD*), a modulator of mineralization (Buchaille et al., 2000; Lin et al., 2019). This same cluster also showed particularly high expression of *COL1A1*. Clusters 2 and 6 expressed high levels of *COCH*, which encodes for a protein involved in mechano-sensation (Goel et al., 2012). Cluster 1 expressed high levels of *DLX5*, while cluster 5 was characterized by high expression of *CTNNB1* and *GOLIM4*. *CTNNB1* codes for b-catenin, key mediator of WNT signaling (Mosimann et al., 2009).

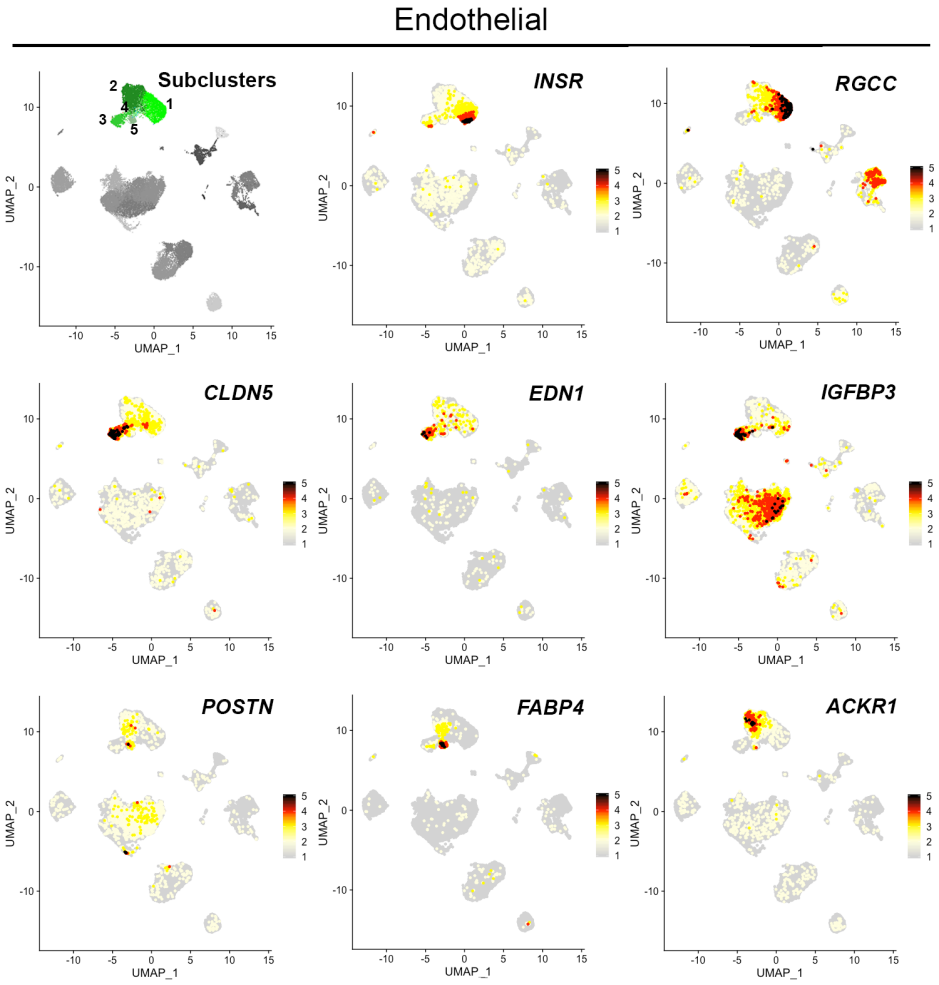

Fig. S4. Feature plots showing the expression of genes characterizing specific subclusters of dental pulp endothelial cells (ECs), related to Figure 1. *INSR* (Insulin Receptor) and *RGCC* marked ECs from subcluster 1. Expression of *INSR* suggests a role for these cells in modulating Glucose and Insulin metabolism within the dental pulp, while *RGCC* expression is usually observed in actively cycling cells (Konishi et al., 2017; Kubota et al., 2011). *CLDN5* (claudin 5), *EDN1* (endothelin 1) and *IGFBP3* were enriched in ECs from cluster 3. These cells co-expressed the arterial markers *GJA5* and *EFNB2 (Mukouyama et al., 2002; Shin et al., 2001)*, thus indicating that this cluster represents arterial ECs. Cluster 5 was characterized by the high expression of *POSTN* (Periostin) and *FABP4,* both associated to angiogenic and pro-survival processes in endothelial cells (Elmasri et al., 2012; Hu et al., 2016). Cluster 2 was marked by the expression of *ACKR1*/*CD234*, which has been proposed as a marker for postcapillary and collecting venules in mice (Thiriot et al., 2017).

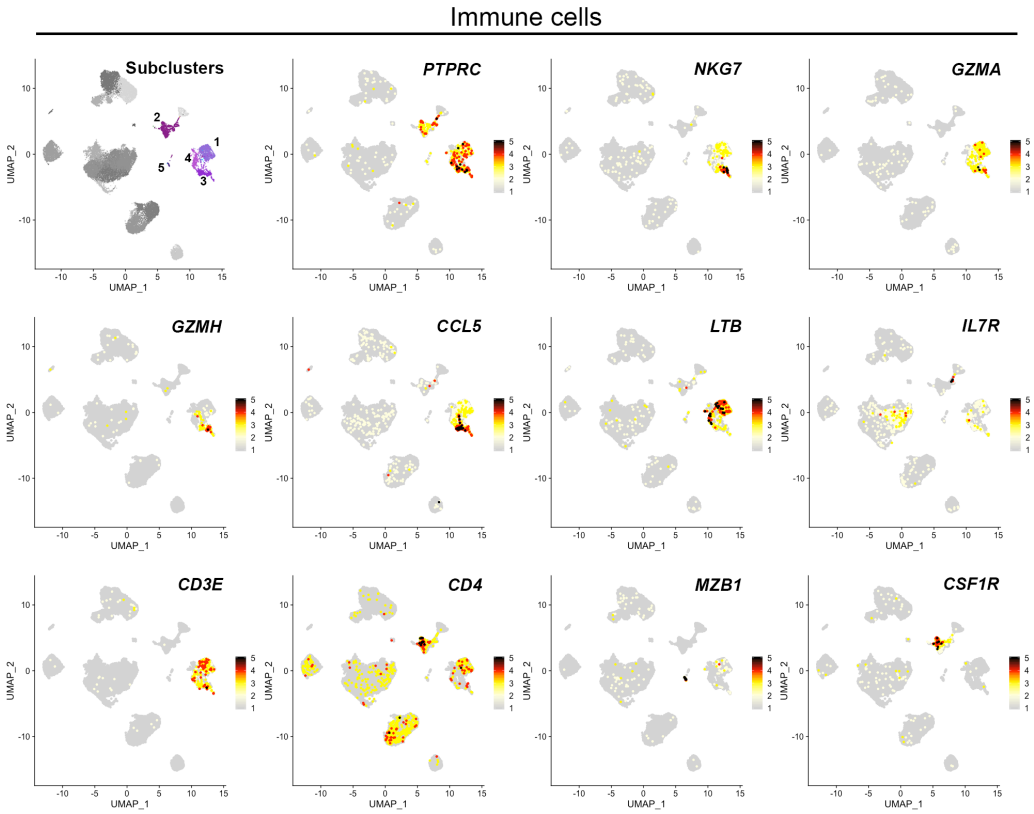

Fig. S5. Feature plots showing the expression of genes characterizing specific subclusters of dental pulp immune cells, related to Figure 1. All immune cells subclusters expressed the immune cells marker *PTPRC* (CD45). Clusters 1, 3 and 4 included T-cells and natural killer cells, as indicated by the expression of *CD3E*, *CD4*, *GZMH*, *GZMA*, and *NKG67.* Cluster 2 included macrophages and monocytes, as indicated by the high expression of CSF1R. Cluster 5 included B cells and plasma cells, as indicated by the expression of *MZB1* and *CD22* (see dataset) (Chetty and Gatter, 1994; Chitu and Stanley, 2006).

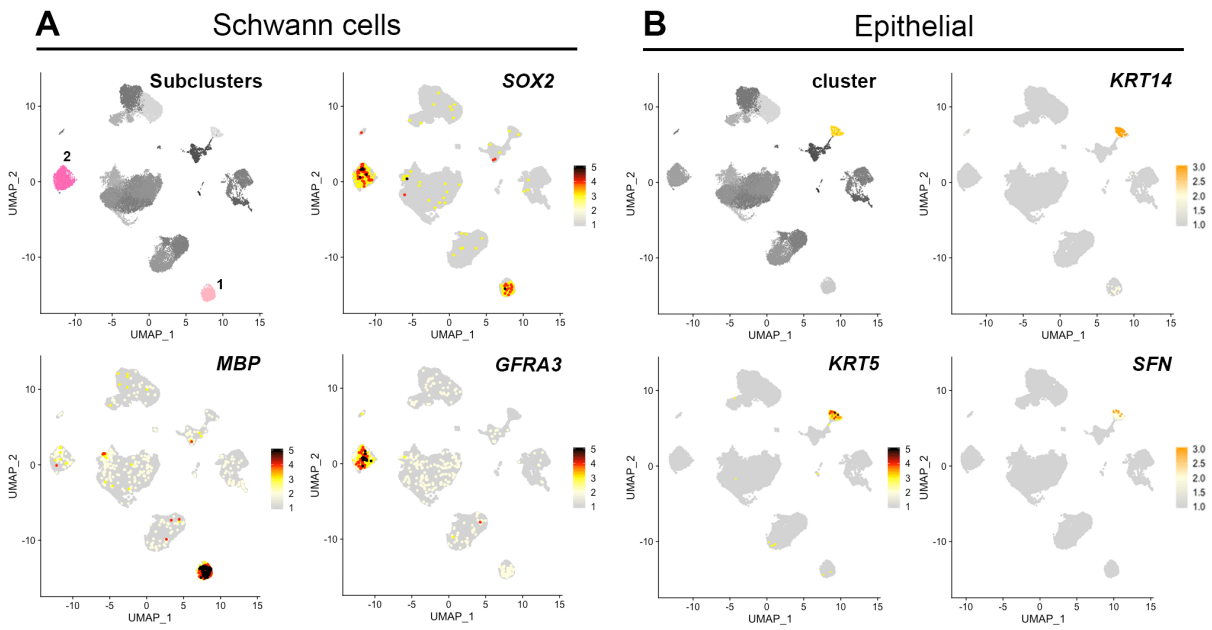

Fig. S6. Feature plots showing the expression of genes characterizing subclusters of dental pulp Schwann cells (A) and epithelial cells (B), related to Figure 1. A) All dental pulp Schwann cells express *SOX2. MBP* (myelin basic protein) is expressed by myelinating Schwann cells, while *GFRA3* (GDNF family receptor alpha-3) marks non-myelinating Schwann cells. B) Epithelial cells express Keratin-coding genes, such as *KRT14* and *KRT5*, as well as Stratifin (*SFN*). Keratins are intermediate filaments, and their expression is mostly restricted to epithelial cells (Herrmann et al., 2007; Karantza, 2011). *SFN* is expressed by differentiated keratinocytes, and it induces activation of adjacent fibroblasts by triggering expression of metalloproteases (Medina et al., 2007).

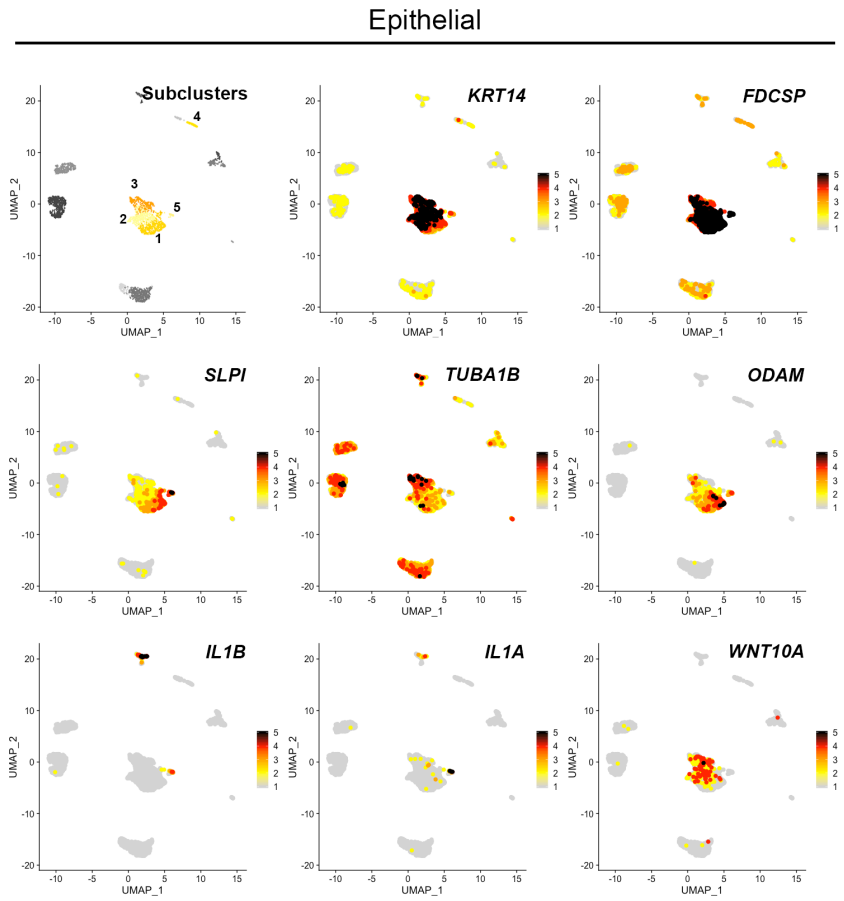

Fig. S7. Feature plots showing the expression of genes characterizing subclusters of periodontal epithelial cells, related to Figure 2. Epithelial cells represent the most abundant cell type in the human periodontium. Epithelial cells have been detected previously in mouse and human periodontal tissues (Athanassiou-Papaefthymiou et al., 2015; Tsunematsu et al., 2016). 5 subclusters could be identified. All epithelial cells express keratin-coding genes such as *KRT14,* and *FDCSP* (Follicular Dendritic Cells Secreted Protein). *KRT14* is a common marker for dental epithelial cells (Tabata et al., 1996). FDCSP increases cell proliferation and inhibits the expression of genes associated with mineralization processes in periodontal MSCs of human teeth (Wei et al., 2011). Subcluster 1 was characterized by the expression of *SLPI* (secretory leukocyte protease inhibitor) and *ODAM* (Odontogenic Ameloblast-associated Protein). *ODAM* is expressed by periodontal epithelial cells that display stem cell properties (Athanassiou-Papaefthymiou et al., 2015). Clusters 2 and 3 showed higher expression of *TUBA1B* (tubulin alpha-1B chain) and *WNT10A. WNT10A* expression in dental epithelium is fundamental for tooth development and root formation (Mues et al., 2014; Yamashiro et al., 2007; Yu et al., 2020; Zhang et al., 2014). Cluster 5 showed higher expression of *IL1A* and *IL1B,* which are fundamental mediators of the immune response against infections (Miller and Cho, 2011), and they are strongly involved in the resolution of periodontal pathologies (Grigoriadou et al., 2010).

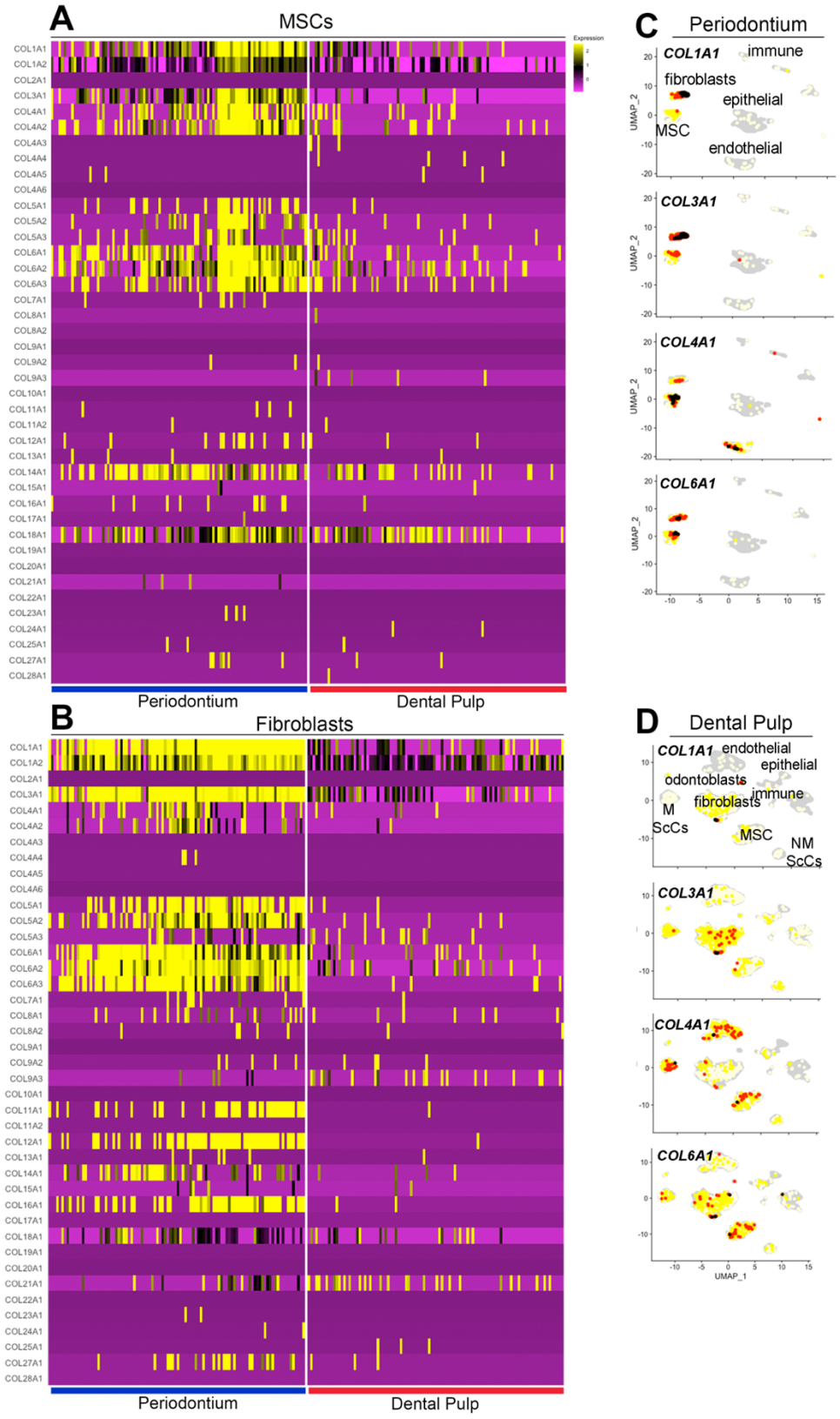

Fig. S8. Expression of collagen-encoding genes, related to Figure 4. A) Heatmap showing differential expression of genes encoding for collagens in MSCs from the periodontium and the dental

pulp. **B)** Heatmap showing differential expression of genes encoding for collagens in fibroblasts from the periodontium and the dental pulp. **C, D)** Feature-plots showing the distribution of collagen-encoding genes in the periodontium (**C**) and in the dental pulp (**D**). Collagen-encoding genes are overall more expressed in the periodontium, in accordance to the intense remodeling that this tissue undergoes in response to mastication.

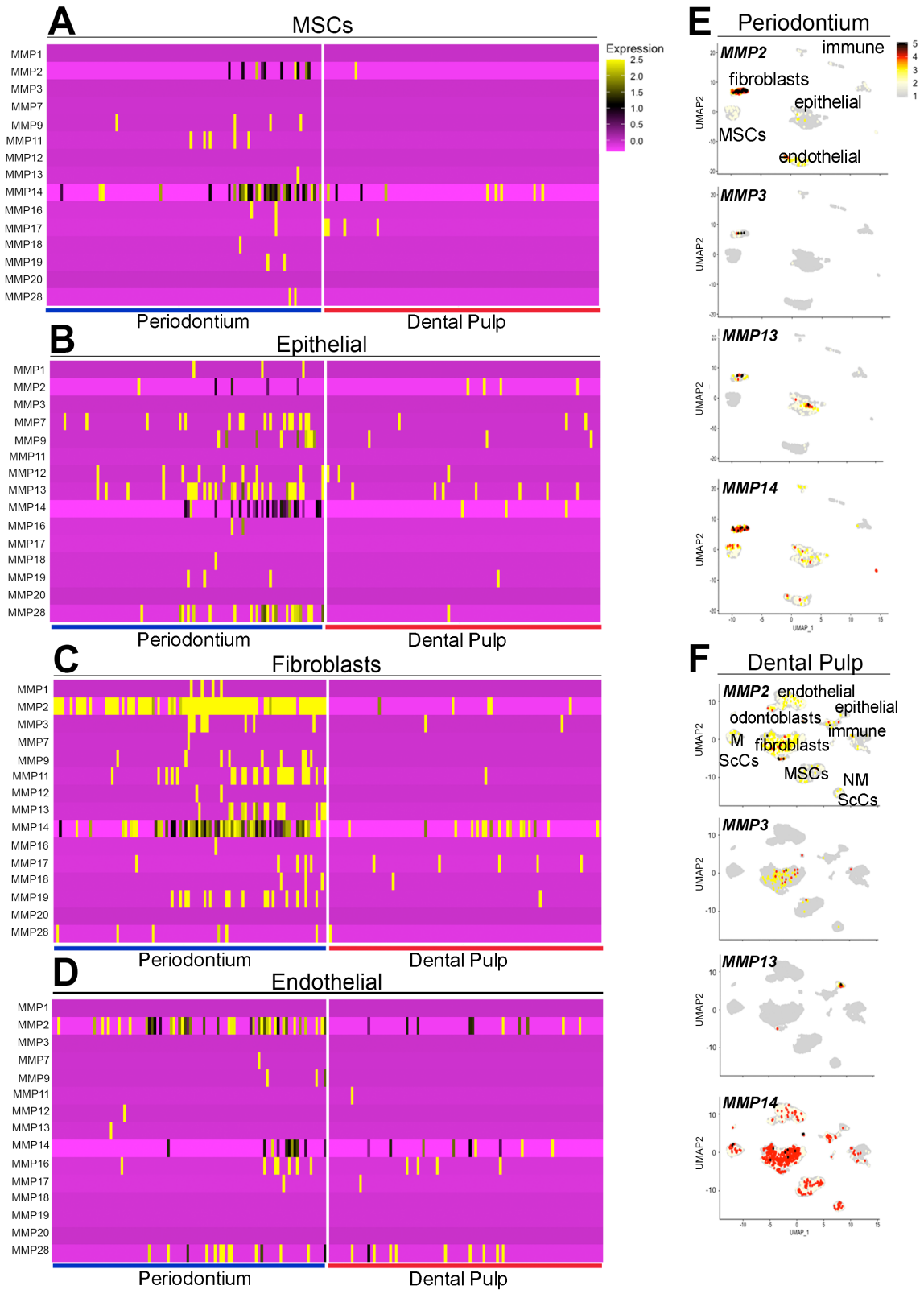

Fig. S9. Expression of genes encoding metalloproteinases (MMPs), related to Figure 4. A-D) Heatmap showing differential expression of genes encoding for MMPs in **A**) MSCs, **B**) epithelial cells, **C**) fibroblasts, **D**) endothelial cells, from the periodontium and the dental pulp. **E, F)** Feature-plots showing the distribution of collagen-encoding genes in the periodontium (**E**) and in the dental

pulp (**F**). MMPs are actively involved in the turnover of the periodontal space since they degrade collagen and most of the secreted proteins that compose the periodontal extracellular matrix (Birkedal-Hansen, 1993; Sapna et al., 2014). *MMPs*-encoding genes are overall more expressed in the periodontium, in accordance with the intense remodeling of the extracellular matrix needed to compensate the stimuli that this tissue receives in response to mastication.

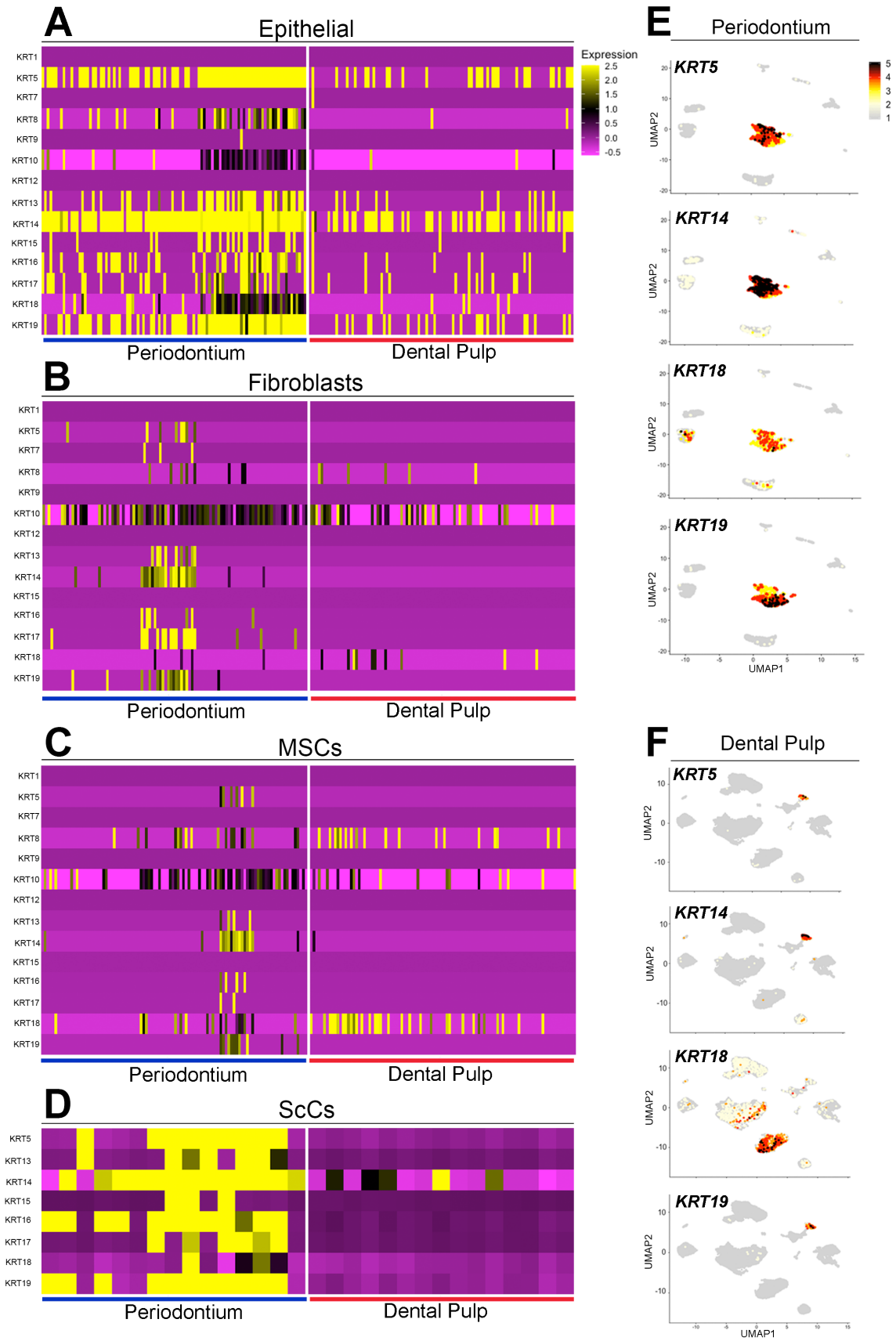

Fig. S10. Expression of genes encoding keratins, related to Figure 4. A-D) Heatmap showing differential expression of genes encoding for keratins in **A**) epithelial cells, **B**) fibroblasts, **C**) MSCs,

D) Schwann cells from the periodontium and the dental pulp. **E, F)** Feature-plots showing the distribution of *Keratin*-encoding genes in the periodontium (**E**) and in the dental pulp (**F**). In the periodontium, *Keratin*-encoding genes are expressed also in non-epithelial cells. *KRT18,* a gene previously reported to be exclusively expressed in cells of single-layered and pseudostratified epithelia (Karantza, 2011), is expressed by MSCs in the dental pulp.

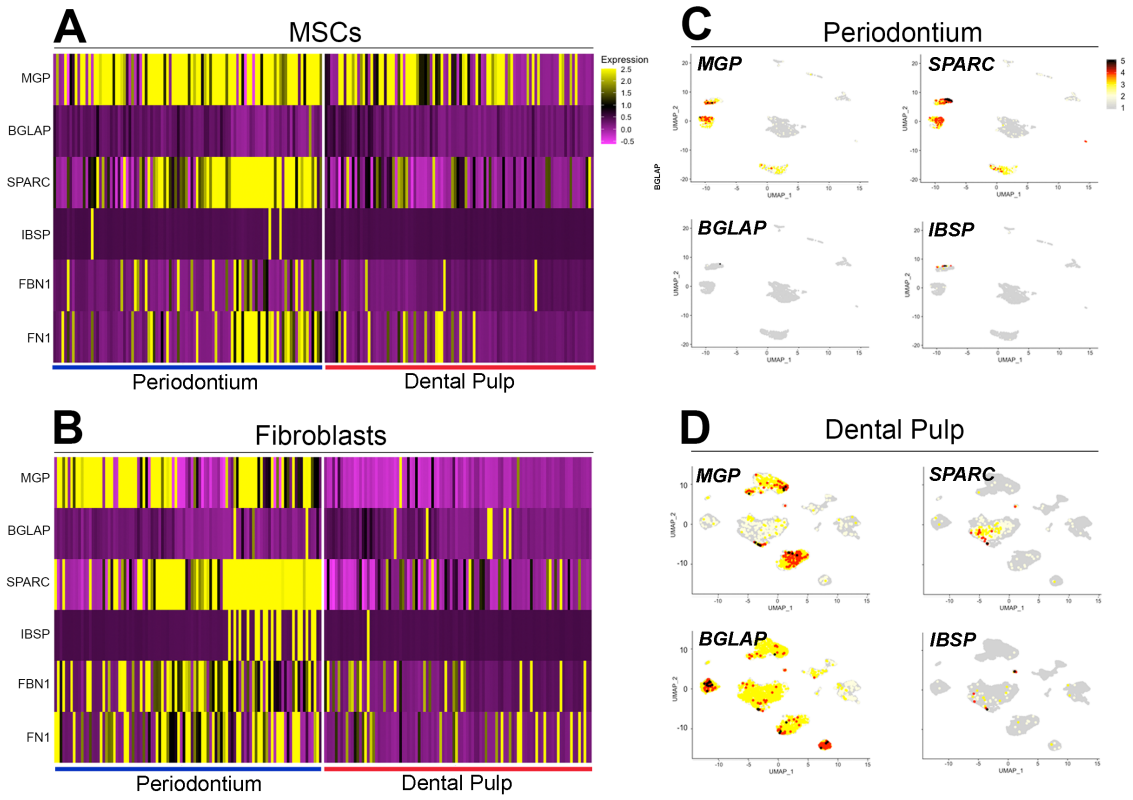

Fig. S11. Expression of genes encoding non-collagenous bone-associated proteins, related to Figure 4. A, B) Heatmaps showing genes differentially expressed between dental pulp and periodontal (**A**) MSCs and (**B**) fibroblasts. **C, D)** Feature plots showing the distribution of gene encoding non-collagenous bone-associated proteins in (**C**) periodontium and (**D**) dental pulp. Periodontal MSCs expressed higher levels of *Osteonectin* (*SPARC*) and *MGP* (Matrix Gla Protein) compared to dental pulp MSCs. Osteonectin is known to regulate Ca^{2+} deposition during bone formation (Termine et al., 1981), but in the periodontium its function is fundamental for proper collagen turnover and organization (Trombetta and Bradshaw, 2010). MGP (Matrix Gla Protein) is a potent inhibitor of mineralization (Kaipatur et al., 2008). Periodontal fibroblasts express higher levels of *SPARC* and *MGP*, as well as *Osteocalcin* (*BGLAP*) and *Bone Sialophosphoprotein* (*BSP*).

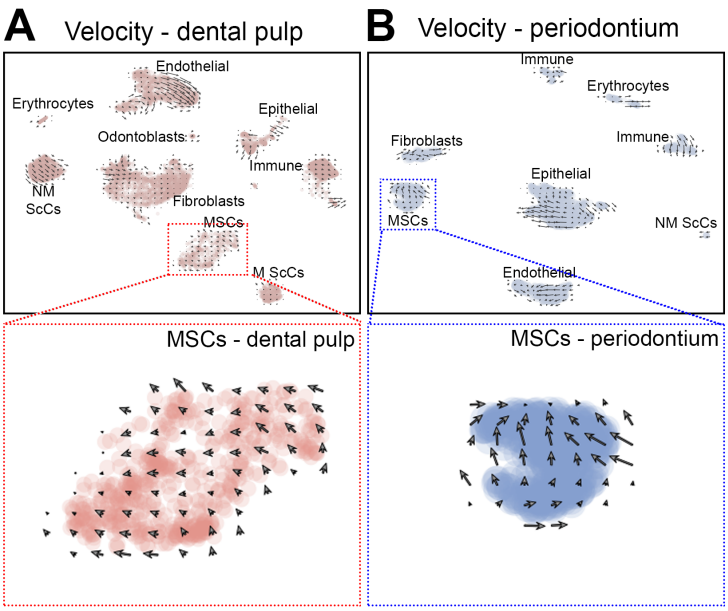

117

118 **Fig. S12. Velocity study of cell trajectories in the dental tissues, related to Figure 3. A)** Velocity
119 in the dental pulp. **B)** Velocity in the periodontium. Red and blue rectangles highlight respectively
120 the dental pulp and periodontal MSCs clusters shown in the global velocity plots. Only patients
121 analyzed with 10X Genomics v3 kit were used in the velocity estimates.

122

123

124

Supplementary Tables

Differential gene expression - Periodontium vs dental pulp MSCs

	gene	p_val	avg_logFC	pct.1	pct.2	p_val_adj
1	HBB	0	3.24581697177998	0.907	0.076	0
2	HBA2	0	2.91169954034701	0.693	0.034	0
3	HBA1	0	2.20113759332632	0.544	0.01	0
4	NNMT	0	1.87850058250694	0.629	0.02	0
5	HOPX	0	1.14458527446871	0.495	0.025	0
6	RPL6P27	6.67256429342861E-267	1.11171714555118	0.742	0.106	1.65993381927623E-262
7	FDCSP	5.94640915612883E-262	2.75087526797022	0.307	0.006	1.47928820577017E-257
8	PTMAP5	1.66832245588792E-243	1.14528932922911	0.633	0.079	4.15028577351238E-239
9	COL3A1	7.52335353873889E-215	1.65707631127883	0.699	0.138	1.87158465983207E-210
10	COL1A1	1.07439383971557E-213	1.59914236139218	0.751	0.162	2.67276955506042E-209
11	SPARCL1	2.99317807053905E-189	1.29053911941933	0.909	0.287	7.44612908607998E-185
12	CXCL12	4.2262140200075E-156	1.19411865882346	0.443	0.064	1.05135526175727E-151
13	IGFBP4	3.92974692001991E-147	1.02031640578958	0.68	0.171	9.77603141293352E-143
14	S100A4	4.38097554588702E-137	1.08885329373367	0.915	0.393	1.08985528655031E-132
15	DCN	3.21450625730978E-126	1.17058089254281	0.67	0.198	7.99672721630954E-122
16	COL6A1	1.9531483174306E-124	1.02344023915478	0.68	0.191	4.8588470692721E-120
17	APOE	2.62528933909972E-108	1.48546734763149	0.695	0.245	6.53093228887836E-104
18	CXCL14	2.21414963747453E-89	-2.04411843929188	0.151	0.606	5.50814005314539E-85
19	SPARC	1.04752798714087E-85	1.00238177918575	0.862	0.481	2.60593537361035E-81
20	IFI27	6.94621489604408E-69	-1.58810329223689	0.328	0.635	1.72800987968888E-64
21	TF	1.08038343540846E-45	-1.51444432023821	0.012	0.325	2.68766987226564E-41
22	KRT18	1.57589643449871E-39	-1.46872929126273	0.157	0.428	3.92035756010244E-35
23	PTN	2.35938566952991E-39	-1.32588047483401	0.414	0.588	5.86944373008955E-35
24	CLU	5.03668354194873E-29	-1.06405551400471	0.212	0.424	1.25297576473059E-24
25	IFI6	3.16052123818713E-28	-1.13704670755114	0.334	0.497	7.86242868423814E-24
26	ISG15	5.16318354573924E-27	-1.28475423457449	0.219	0.415	1.28444517067355E-22
27	RBP1	1.78272016950256E-24	-1.05038498240697	0.058	0.253	4.43487296567152E-20
28	RARRES1	2.5228534697408E-21	-1.00182017404775	0.008	0.172	6.27610257667419E-17
29	PTGDS	5.07390837482826E-20	-1.01012662211226	0.027	0.189	1.26223618640603E-15
30	IGFBP6	6.09168123937234E-19	-1.0714522518631	0.264	0.403	1.51542754191866E-14
31	RHOB	6.15620502917967E-15	-1.03599434939694	0.328	0.419	1.53147912510903E-10
32	PPP1CB	7.01853477480945E-11	-1.06066566583755	0.454	0.465	1.74600089592935E-06
33	DDIT4	1.0355171449118E-10	-1.03502796781716	0.198	0.302	2.5760560013971E-06

Table S1. Genes differentially expressed (Fc > 1; p < 0.005) between periodontal and dental pulp MSCs, related to Figure 3. Periodontal MSCs expressed higher levels of *CCL2* and *Collagen* encoding genes. Periodontal MSCs were also characterized by higher expression of *SPARC*/*Osteonectin,* a secreted molecule fundamental for the regulation of periodontal homeostasis and Collagen content (Trombetta and Bradshaw, 2010). Dental pulp MSCs expressed higher levels of *CXCL14,* is associated with increased angiogenic potential (Hayashi et al., 2015), and *RARRES1* which mediates retinoic acid-responses in stem cells (Oldridge et al., 2013). Dental pulp MSCs

strongly expressed *KRT18,* a gene previously reported to be exclusively expressed in cells of single-layered and pseudostratified epithelia (Omary et al., 2009).

Pairwise extended jaccard similarity - ranks

	Cell type 1	Cell type 2
1	Epithelial_perio	Myelinating_ScCs perio
2	Endothelial_perio	Endothelial_pulp
3	Erythrocytes_perio	Erythrocytes_pulp
4	MSC_perio	MSC_pulp
5	Non-Myelinating_ScCs_pulp	Myelinating_ ScCs_pulp
6	Epithelial_pulp	Myelinating_ScCs_perio
7	Odontoblasts_pulp	Fibroblasts_pulp
8	Fibroblasts_perio	Cementoblasts_perio
9	Non-Myelinating ScCs_perio	Non-Myelinating_ ScCs_pulp
10	Immune_perio	Immune_pulp

Number of DEG - cell type

	cell types	Number of DEG
1	MSC	333
2	Fibroblasts	688
3	Erythrocytes	125
4	Epithelial	545
5	Immune	351
6	Endothelial	475
7	Non-Myelinating ScCs	143
8	Odontoblasts / Cementoblasts	107
9	Myelinating ScCs	313

Table S2, related to Figure 4. Left: Periodontal and dental pulp cell types ranked according to pairwise extended jaccard similarity. Right: number of differentially expressed genes between equivalent cell types in the dental pulp and the periodontium

Collagen-encoding genes

(Periodontium vs dental pulp)

Fibroblasts

	gene	p_val	avg_logFC	pct.1	pct.2	p_val_adj
111	COL1A1	2.25487242834546E-166	3.3019368581082	0.928	0.376	5.60944613999501E-162
189	COL1A2	5.24386883102724E-106	1.96956844269406	0.975	0.737	1.30451724909465E-101
120	COL3A1	2.22198351415981E-153	2.40575302329749	0.957	0.495	5.52762838817536E-149
105	COL4A1	7.45156869789291E-180	0.83048292325594	0.343	0.027	1.85372674497482E-175
123	COL4A2	1.71151093270727E-150	0.712807129120808	0.379	0.04	4.25772574729587E-146
17	COL5A1	0	1.22445080957512	0.632	0.03	0
75	COL5A2	3.05331225252665E-254	1.23286104790791	0.733	0.092	7.59572489061056E-250
72	COL6A1	9.39035086594511E-259	1.74716413138289	0.866	0.144	2.33603758492117E-254
89	COL6A2	3.43727039099989E-206	1.89125151813711	0.924	0.241	8.55089755169042E-202
6	COL6A3	0	1.82762970827482	0.834	0.075	0
635	COL9A3	1.03141268744368E-09	-0.643726096050555	0.043	0.18	2.56584534255364E-05
16	COL11A1	0	1.27768783976508	0.444	0.013	0
12	COL12A1	0	1.53579904694227	0.61	0.006	0
20	COL14A1	0	1.1029391222703	0.455	0.019	0
23	COL16A1	0	1.02744676887705	0.538	0.026	0
476	COL18A1	2.47330333647109E-32	0.254176480519037	0.419	0.139	6.15283671013913E-28
937	COL21A1	0.115313439128048	-0.484816613063316	0.213	0.219	1

MSCs

	gene	p_val	avg_logFC	pct.1	pct.2	p_val_adj
12	COL1A1	1.07439383971557E-213	1.59914236139218	0.751	0.162	2.67276955506042E-209
189	COL1A2	4.7454973002183E-46	0.728211899450018	0.732	0.399	1.18053736337531E-41
11	COL3A1	7.52335353873889E-215	1.65707631127883	0.699	0.138	1.87158465983207E-210
53	COL4A1	8.8143610293432E-103	0.860257329496067	0.495	0.118	2.19274859326971E-98
120	COL4A2	3.05435194531821E-66	0.568640888255137	0.555	0.192	7.59831133436812E-62
60	COL5A1	6.68949374408408E-95	0.327013912144249	0.216	0.021	1.6641453587158E-90
92	COL5A2	2.17400695967927E-76	0.484278088748829	0.338	0.07	5.40827711359411E-72
32	COL6A1	1.9531483174306E-124	1.02344023915478	0.68	0.191	4.8588470692721E-120
72	COL6A2	4.42759676271991E-89	0.831620893206911	0.744	0.292	1.10145324666183E-84
41	COL6A3	2.15934421027835E-115	0.706814172812724	0.532	0.119	5.37180059190944E-111
105	COL14A1	9.36381906188564E-70	0.505434369436353	0.647	0.227	2.32943726802529E-65
57	COL16A1	6.58947716426885E-100	0.344835214148013	0.169	0.01	1.63926423415516E-95

Table S3. Collagen-encoding genes differentially expressed (p < 0.001) between periodontal and dental pulp fibroblasts and MSCs, related to Figure 3 and Figure 4.

Keratin-encoding genes

(Periodontium vs dental pulp)

Epithelial

	gene	p_val	avg_logFC	pct.1	pct.2	p_val_adj
51	KRT5	1.7760833374321E-50	0.662134563892527	0.773	0.269	4.41836251852985E-46
21	KRT8	1.95430325171363E-55	0.296545123782922	0.423	0.035	4.861720199288E-51
117	KRT13	2.40526568560614E-37	0.489124101031112	0.478	0.115	5.9835794460824E-33
104	KRT14	9.53489912531268E-40	0.512019219754885	0.954	0.551	2.37199685540404E-35
237	KRT15	1.06289366570786E-21	0.327423789729451	0.211	0.03	2.64416057218144E-17
27	KRT18	2.37494190777221E-54	0.371834626953621	0.466	0.057	5.90814298396493E-50
15	KRT19	2.91730913531038E-57	0.770694899057093	0.792	0.272	7.25738993591163E-53
211	KRT8	1.95430325171363E-55	0.296545123782922	0.423	0.035	4.861720199288E-51

MSCs

	gene	p_val	avg_logFC	pct.1	pct.2	p_val_adj
306	KRT8	8.17811740716836E-12	-0.788924436402796	0.107	0.224	2.03447026738127E-07
56	KRT14	1.02735136523106E-100	0.489689085742613	0.132	0.004	2.55574199128531E-96
220	KRT18	1.57589643449867E-39	-1.46872929126273	0.157	0.428	3.92035756010235E-35
3061	KRT8	8.17811740716836E-12	-0.788924436402796	0.107	0.224	2.03447026738127E-07

Fibroblasts

	gene	p_val	avg_logFC	pct.1	pct.2	p_val_adj
33	KRT14	0	0.774716256198696	0.224	0.003	0
63	KRT17	2.6869875919885E-296	0.310658566332385	0.148	0.001	6.6844190325898E-292

ScCs

	gene	p_val	avg_logFC	pct.1	pct.2	p_val_adj
10	KRT5	9.49024512712327E-177	2.30252721192442	0.538	0.002	2.36088828027446E-172
125	KRT8	3.98619631248065E-32	0.803345311854587	0.333	0.02	9.91646056655812E-28
903	KRT10	0.136263579018209	-0.275482038836599	0.41	0.25	1
22	KRT13	4.97856780968926E-141	2.10478124975943	0.359	0	1.2385183140164E-136
156	KRT14	1.58832510524415E-20	2.80853628699739	0.667	0.177	3.95127636431588E-16
95	KRT15	2.5345804340202E-51	0.326997146876151	0.128	0	6.30527574571206E-47
16	KRT16	2.05969189935912E-161	2.31989135139677	0.436	0.001	5.12389553803569E-157
75	KRT17	1.72889343997505E-62	0.77870053053477	0.231	0.002	4.30096821062594E-58
193	KRT18	2.92626668227313E-13	0.498738700096318	0.282	0.037	7.27967362549086E-09
5	KRT19	7.38677820170057E-193	2.87943743216864	0.538	0.001	1.83760881323705E-188
1251	KRT8	3.98619631248065E-32	0.803345311854587	0.333	0.02	9.91646056655812E-28

Table S4. Keratin-encoding genes differentially expressed (p < 0.001) between periodontal and dental pulp epithelial cells, MSCs, fibroblasts and ScCs, related to Figure 3 and Figure 4.

MMP-encoding genes

(Periodontium vs dental pulp)

Fibroblasts

	gene	p_val	avg_logFC	pct.1	pct.2	p_val_adj
67	MMP2	4.6148452189556E-282	1.9538842190864	0.83	0.124	1.14803504511958E-277
118	MMP11	3.64223980263109E-156	0.265536622985388	0.206	0.01	9.06079995700536E-152
11	MMP13	0	1.54239457203761	0.191	0	0
319	MMP14	5.78794888219009E-62	0.471100307125854	0.61	0.178	1.43986804342243E-57

Epithelial

	gene	p_val	avg_logFC	pct.1	pct.2	p_val_adj
256	MMP7	1.93984660931978E-20	0.335364772334984	0.196	0.027	4.82575641000482E-16
423	MMP12	2.90533031306277E-11	0.319730178933507	0.129	0.027	7.22759021980626E-07
175	MMP13	1.55228121633805E-26	0.553801448188468	0.28	0.049	3.86160998188416E-22

Endothelial

	gene	p_val	avg_logFC	pct.1	pct.2	p_val_adj
7	MMP2	1.30077357343548E-131	0.595358740089258	0.386	0.066	3.23593441863545E-127

Table S5. Genes encoding for metalloproteases (MMP) differentially expressed ($p < 0.001$) between periodontal and dental pulp fibroblasts, epithelial cells, and endothelial cells, related to Figure 4.

Non collagenous bone-associated proteins
(periodontium vs dental pulp)

Fibroblasts

	gene	p_val	avg_logFC	pct.1	pct.2	p_val_adj
81	MGP	1.78588906938445E-219	1.99197028249637	0.805	0.141	4.4427562379077E-215
213	SPARC	5.16602480192375E-94	1.94575060495438	0.877	0.515	1.28515198997457E-89
73	IBSP	1.93163964632213E-255	1.46661576267429	0.181	0.003	4.80533994815555E-251
343	FBN1	7.1117677680317E-58	0.533218478334099	0.625	0.192	1.76919446765325E-53
330	FN1	2.98712269762832E-60	0.581968071589218	0.632	0.194	7.43106513488997E-56

MSCs

	gene	p_val	avg_logFC	pct.1	pct.2	p_val_adj
233	MGP	8.87543348342118E-37	0.501073027684103	0.874	0.545	2.20794158767069E-32
80	SPARC	1.04752798714087E-85	1.00238177918576	0.862	0.481	2.60593537361035E-81

Table S6. Genes encoding for non-collagenous bone associated-proteins differentially expressed ($p < 0.001$) between periodontal and dental pulp fibroblasts and MSCs, related to Figure 3 and Figure 4.

Transparent methods

Resource availability

The accession number for all sequencing data reported in this paper is GEO: GSE161267. All code is publicly available at: https://github.com/TheMoorLab/Tooth

Experimental model and subject details

The procedure for the collection of anonymized human dental pulp and periodontal cells at the Center of Dental Medicine (ZZM) of the University of Zurich was approved by the Ethic Commission of the Kanton of Zurich (reference number 2012-0588) and the patients gave their written informed consent. Samples were obtained in fully anonymized form from patients of 18-35 years of age.

Method details, quantification and statistical analysis

Isolation of cells from the dental pulp and the periodontium for single cell RNA sequencing. Tooth extractions were performed by professional dentists at the Oral Surgery department of ZZM of the University of Zurich. Evaluation of the health status of the tooth was done post-extraction, upon direct observation of the specimen. All procedures were performed in accordance with the current guidelines. Teeth were collected immediately after extraction and preserved in sterile NaCl 0.9%, on ice for the time needed to transfer them from the clinic to the processing laboratory (< 10 minutes). The periodontium was isolated by scratching the lower two-thirds of the root of the teeth with a surgical scalpel directly into a Petri dish filled with sterile, cold Hank's Balanced Salt Solution

(HBSS; Thermo Fisher Scientific, Reinach, Switzerland). The upper-third of the root was excluded to minimize contamination from the gingival epithelium. The cleansed tooth was then carefully wiped with 70% ethanol. The tooth was then cracked with a press, and carefully opened with forceps. The dental pulp was then removed from the tooth with a separate set of instruments, placed in a Petri dish filled with cold HBSS and minced into small pieces (< 2 mm diameter). Thereafter, periodontal and pulp tissues were transferred in falcon tubes filled with HBSS, centrifuged at 4°C, 300g, for 10 minutes. Tissues were digested in 10 mL Collagenase P 5 U/mL (11 213 873 001, Sigma Aldrich, Buchs, Switzerland) for 40 minutes at 37°C. After digestion, samples were disaggregated by pipetting, filtered through a 70 µm cell strainer, and resuspended in HBSS + 0.002% Bovine Serum Albumin (BSA; 0163.2, Roth AG, Arlesheim, Switzerland).

Single-cell RNA sequencing (scRNA-seq) using 10X Genomics platform. The quality and concentration of the single cell preparations were evaluated using a hemocytometer in a Leica DM IL LED microscope and adjusted to 1'000 cells/µl. 10'000 cells per sample were loaded into the 10X Chromium controller and library preparation was performed according to the manufacturer's indications (single cell 3' v2 or v3 protocol). The resulting libraries were sequenced in an Illumina NovaSeq sequencer according to 10X Genomics recommendations (paired end reads, R1=26, i7=8, R2=98) to a depth of around 50.000 reads per cell.

Computational analysis. Velocity analysis was performed using scVelo (Bergen et al., 2019) and Python v3.6. Velocity was only calculated for patients' samples sequenced with 10X v3. All other data analysis was performed using Seurat v3 (Stuart et al., 2019) and R version 3.6.4. Clusters were visualized using uniform manifold approximation and projection (UMAP) (McInnes et al., 2018). Dental pulp and periodontium data were initially analyzed separately. Data was scaled and transformed using SCTransform (Hafemeister and Satija, 2019) for variance stabilization. Analysis of merged dental pulp and periodontium data was performed by integrating data with R package Harmony (Korsunsky et al., 2019) to cluster data into cell types. Any subsequent analysis was done using raw data and not data transformed after integration. In particular, all statistical analysis of differential expression was performed on unintegrated and untransformed data as both could lead to dependencies in the data rendering the assumption of independence of the statistical test void. Differential expression analysis was performed using the Wilcoxon rank sum test. All p values reported were adjusted for multiple comparisons using the Bonferroni correction. The extended Jaccard similarity was computed on the top three thousand differentially expressed genes across the two datasets (pulp and perio samples).

Processing of human teeth for immunofluorescent staining. Teeth used for histological analysis and immunostaining were immediately fixed by immersion in paraformaldehyde 4% (PFA 4%) for 24 hours, then decalcified in Morse's solution for 8 weeks, dehydrated, embedded in paraffin, and serially sectioned at 5 µm. From a subset of teeth, the dental pulp was immediately extracted and fixed in PFA 4% for 2 hours. The specimens were then incubated in Sucrose 30%, embedded in Tissue Tek® O.C.T.™ (4583, Sakura, Alphen aan den Rijn, Netherlands), and serially sectioned at 10 µm.

Immunostaining. Paraffin sections were rehydrated by incubation in Xylol followed by a series of Ethanol solutions (100% to 30%) and distilled H_2O. Cryosections were let dry at room temperature for 1 hour and then washed with PBS before immunostaining. Cells used for immunofluorescent staining were first fixed in PFA 4% for 15 minutes at 4°C. Thereafter, specimens were blocked with PBS supplemented with 2% Fetal Bovine Serum (FBS) and incubated with primary antibodies for 1 hour at room temperature. The following primary antibodies were used: Rabbit anti-Keratin 14 (1:500; PRB-155P, BioLegend, San Diego, CA, U.S.A.), Mouse anti-Vimentin (1:100; M0725, Dako, Baar, Switzerland), Mouse anti-FRZB (1:50, LS-B6898-50, LSBio, Seattle, WA, U.S.A.), Rabbit anti-Dentin Sialophosphoprotein (DSPP) (1:100, ENH083, Kerafast, Boston, MA, U.S.A.), Rabbit anti-Laminin (1:20; ab11575, Abcam, Cambridge, United Kingdom), anti-MBP (1:200; MAB386, Millipore), anti-CD31 (1:50; ab28364, Abcam, Cambridge, UK), anti-CD234 (1:50; 566424, BD, Eysin Switzerland), anti-CD31 (1:20, ab28364, Abcam, Cambridge, UK). The sections were then incubated with Fluorochrome-conjugated secondary antibodies for 1 hour at room temperature at dark. The following secondary antibodies were used: Alexa-568 Donkey anti-Rabbit (1:500; A10042, Thermo Fisher Scientific, Reinach, Switzerland), Alexa-488 Chicken anti-Goat (1:500; A-21467, Thermo Fisher Scientific, Reinach, Switzerland), Alexa-488 Goat anti-Rabbit (1:500; A32731, Thermo Fisher Scientific, Reinach, Switzerland), Alexa-568 Goat anti-Rat (1:500; A-11077, Thermo Fisher Scientific, Reinach, Switzerland). DAPI (4',6-Diamidino-2-Phenylindole; D1306, Thermo Fisher Scientific, Reinach, Switzerland) was then used for nuclear staining. After immunofluorescent staining, samples were mounted in ProLong™ Diamond Antifade Mountant (P36965, Thermo Fisher Scientific, Reinach, Switzerland), and imaged with a Leica SP8 Inverted Confocal Laser Scanning Microscope (Leica Microsystems- Schweiz AG, Heerbrugg, Switzerland).

KEY RESOURCES TABLE

REAGENT or RESOURCE	SOURCE	IDENTIFIER
Antibodies		
anti-Keratin 14	BioLegend	Cat#PRB-155P
anti-Vimentin	Agilent/DAKO	Cat#M0725
Anti-DSPP	Kerafast	Cat#ENH083
Anti-GFRA3	Abcam	Cat#ab8028
Anti-MBP	Millipore	Cat#MAB386
Anti-CD31	Abcam	Cat#ab28364
Anti-Laminin	Abcam	Cat#ab11575
Anti-CD234	BD	Cat#566424
Anti-FRZB	LSBio	Cat#LS-B6898-50
Bacterial and Virus Strains		
nn		
Biological Samples		
Human teeth	Center of Dental Medicine, University of Zurich, Zurich, Switzerland	nn
Chemicals, Peptides, and Recombinant Proteins		
nn		
Critical Commercial Assays		
nn		
Deposited Data		
Raw and analyzed data	This paper	GEO: GSE161267
Experimental Models: Cell Lines		
nn		
Experimental Models: Organisms/Strains		

Oligonucleotides		
nn		
Recombinant DNA		
nn		
Software and Algorithms		
ImageJ	Schneider et al., 2012	https://imagej.nih.gov/ij/
Seurat v3	Stuart et. Al. 2019	https://satijalab.org/seurat/v3.0/integration.html
R Package Harmony	Korsunsky et al., 2019	https://github.com/immunogenomics/harmony
R Package NicheNet	Browaeys et al. 2020	https://github.com/saeyslab/nichenetr
R version 3.6.4	R Project	https://cran.r-project.org/bin/windows/base/old/3.6.4/
Other		
nn		

257
258
259
260
261
262
263
264
265
266
267

Supplementary references

Athanassiou-Papaefthymiou, M., Papagerakis, P., and Papagerakis, S. (2015). Isolation and Characterization of Human Adult Epithelial Stem Cells from the Periodontal Ligament. J Dent Res *94*, 1591-1600.

Bergen, V., Lange, M., Peidli, S., Wolf, F.A., and Theis, F.J. (2019). Generalizing RNA velocity to transient cell states through dynamical modeling. BioRxiv.

Birkedal-Hansen, H. (1993). Role of Matrix Metalloproteinases in Human Periodontal Diseases. J Periodontol *64 Suppl 5S*, 474-484.

Buchaille, R., Couble, M.L., Magloire, H., and Bleicher, F. (2000). Expression of the small leucine-rich proteoglycan osteoadherin/osteomodulin in human dental pulp and developing rat teeth. Bone *27*, 265-270.

Chetty, R., and Gatter, K. (1994). CD3: structure, function, and role of immunostaining in clinical practice. J Pathol *173*, 303-307.

Chitu, V., and Stanley, E.R. (2006). Colony-stimulating factor-1 in immunity and inflammation. Curr Opin Immunol *18*, 39-48.

Elmasri, H., Ghelfi, E., Yu, C.W., Traphagen, S., Cernadas, M., Cao, H., Shi, G.P., Plutzky, J., Sahin, M., Hotamisligil, G.*, et al.* (2012). Endothelial cell-fatty acid binding protein 4 promotes angiogenesis: role of stem cell factor/c-kit pathway. Angiogenesis *15*, 457-468.

Goel, M., Sienkiewicz, A.E., Picciani, R., Wang, J., Lee, R.K., and Bhattacharya, S.K. (2012). Cochlin, intraocular pressure regulation and mechanosensing. PLoS One *7*, e34309.

Grigoriadou, M.E., Koutayas, S.O., Madianos, P.N., and Strub, J.R. (2010). Interleukin-1 as a genetic marker for periodontitis: review of the literature. Quintessence Int *41*, 517-525.

Hafemeister, C., and Satija, R. (2019). Normalization and variance stabilization of single-cell RNA-seq data using regularized negative binomial regression. bioRxiv, 576827.

Hayashi, Y., Murakami, M., Kawamura, R., Ishizaka, R., Fukuta, O., and Nakashima, M. (2015). CXCL14 and MCP1 are potent trophic factors associated with cell migration and angiogenesis leading to higher regenerative potential of dental pulp side population cells. Stem Cell Res Ther *6*, 111.

Herrmann, H., Bar, H., Kreplak, L., Strelkov, S.V., and Aebi, U. (2007). Intermediate filaments: from cell architecture to nanomechanics. Nat Rev Mol Cell Biol *8*, 562-573.

Hu, F., Shang, X.F., Wang, W., Jiang, W., Fang, C., Tan, D., and Zhou, H.C. (2016). High-level expression of periostin is significantly correlated with tumour angiogenesis and poor prognosis in osteosarcoma. Int J Exp Pathol *97*, 86-92.

Kaipatur, N.R., Murshed, M., and McKee, M.D. (2008). Matrix Gla protein inhibition of tooth mineralization. J Dent Res *87*, 839-844.

Karantza, V. (2011). Keratins in health and cancer: more than mere epithelial cell markers. Oncogene *30*, 127-138.

Konishi, M., Sakaguchi, M., Lockhart, S.M., Cai, W., Li, M.E., Homan, E.P., Rask-Madsen, C., and Kahn, C.R. (2017). Endothelial insulin receptors differentially control insulin signaling kinetics in peripheral tissues and brain of mice. Proc Natl Acad Sci U S A *114*, E8478-E8487.

Korsunsky, I., Millard, N., Fan, J., Slowikowski, K., Zhang, F., Wei, K., Baglaenko, Y., Brenner, M., Loh, P.R., and Raychaudhuri, S. (2019). Fast, sensitive and accurate integration of single-cell data with Harmony. Nat Methods *16*, 1289-1296.

Kubota, T., Kubota, N., Kumagai, H., Yamaguchi, S., Kozono, H., Takahashi, T., Inoue, M., Itoh, S., Takamoto, I., Sasako, T.*, et al.* (2011). Impaired insulin signaling in endothelial cells reduces insulin-induced glucose uptake by skeletal muscle. Cell Metab *13*, 294-307.

Lin, W., Gao, L., Jiang, W., Niu, C., Yuan, K., Hu, X., Ma, R., and Huang, Z. (2019). The role of osteomodulin on osteo/odontogenic differentiation in human dental pulp stem cells. BMC Oral Health *19*, 22.

McInnes, L., Healy, J., Saul, N., and Grossberger, L. (2018). UMAP: Uniform Manifold Approximation and Projection. Journal of Open Access Software *3*, 861.
Medina, A., Ghaffari, A., Kilani, R.T., and Ghahary, A. (2007). The role of stratifin in fibroblast-keratinocyte interaction. Mol Cell Biochem *305*, 255-264.
Miller, L.S., and Cho, J.S. (2011). Immunity against Staphylococcus aureus cutaneous infections. Nat Rev Immunol *11*, 505-518.
Mitsiadis, T.A., Salmivirta, M., Muramatsu, T., Muramatsu, H., Rauvala, H., Lehtonen, E., Jalkanen, M., and Thesleff, I. (1995). Expression of the heparin-binding cytokines, midkine (MK) and HB-GAM (pleiotrophin) is associated with epithelial-mesenchymal interactions during fetal development and organogenesis. Development *121*, 37-51.
Mosimann, C., Hausmann, G., and Basler, K. (2009). Beta-catenin hits chromatin: regulation of Wnt target gene activation. Nat Rev Mol Cell Biol *10*, 276-286.
Mues, G., Bonds, J., Xiang, L., Vieira, A.R., Seymen, F., Klein, O., and D'Souza, R.N. (2014). The WNT10A gene in ectodermal dysplasias and selective tooth agenesis. Am J Med Genet A *164A*, 2455-2460.
Mukouyama, Y.S., Shin, D., Britsch, S., Taniguchi, M., and Anderson, D.J. (2002). Sensory nerves determine the pattern of arterial differentiation and blood vessel branching in the skin. Cell *109*, 693-705.
Oldridge, E.E., Walker, H.F., Stower, M.J., Simms, M.S., Mann, V.M., Collins, A.T., Pellacani, D., and Maitland, N.J. (2013). Retinoic acid represses invasion and stem cell phenotype by induction of the metastasis suppressors RARRES1 and LXN. Oncogenesis *2*, e45.
Omary, M.B., Ku, N.O., Strnad, P., and Hanada, S. (2009). Toward unraveling the complexity of simple epithelial keratins in human disease. J Clin Invest *119*, 1794-1805.
Sapna, G., Gokul, S., and Bagri-Manjrekar, K. (2014). Matrix metalloproteinases and periodontal diseases. Oral Dis *20*, 538-550.
Shin, D., Garcia-Cardena, G., Hayashi, S., Gerety, S., Asahara, T., Stavrakis, G., Isner, J., Folkman, J., Gimbrone, M.A., Jr., and Anderson, D.J. (2001). Expression of ephrinB2 identifies a stable genetic difference between arterial and venous vascular smooth muscle as well as endothelial cells, and marks subsets of microvessels at sites of adult neovascularization. Dev Biol *230*, 139-150.
Stuart, T., Butler, A., Hoffman, P., Hafemeister, C., Papalexi, E., Mauck, W.M., 3rd, Hao, Y., Stoeckius, M., Smibert, P., and Satija, R. (2019). Comprehensive Integration of Single-Cell Data. Cell *177*, 1888-1902 e1821.
Tabata, M.J., Matsumura, T., Liu, J.G., Wakisaka, S., and Kurisu, K. (1996). Expression of cytokeratin 14 in ameloblast-lineage cells of the developing tooth of rat, both in vivo and in vitro. Arch Oral Biol *41*, 1019-1027.
Termine, J.D., Kleinman, H.K., Whitson, S.W., Conn, K.M., McGarvey, M.L., and Martin, G.R. (1981). Osteonectin, a bone-specific protein linking mineral to collagen. Cell *26*, 99-105.
Thiriot, A., Perdomo, C., Cheng, G., Novitzky-Basso, I., McArdle, S., Kishimoto, J.K., Barreiro, O., Mazo, I., Triboulet, R., Ley, K.*, et al.* (2017). Differential DARC/ACKR1 expression distinguishes venular from non-venular endothelial cells in murine tissues. BMC Biol *15*, 45.
Trombetta, J.M., and Bradshaw, A.D. (2010). SPARC/osteonectin functions to maintain homeostasis of the collagenous extracellular matrix in the periodontal ligament. J Histochem Cytochem *58*, 871-879.
Tsunematsu, T., Fujiwara, N., Yoshida, M., Takayama, Y., Kujiraoka, S., Qi, G., Kitagawa, M., Kondo, T., Yamada, A., Arakaki, R.*, et al.* (2016). Human odontogenic epithelial cells derived from epithelial rests of Malassez possess stem cell properties. Lab Invest *96*, 1063-1075.
Wei, N., Yu, H., Yang, S., Yang, X., Yuan, Q., Man, Y., and Gong, P. (2011). Effect of FDC-SP on the phenotype expression of cultured periodontal ligament cells. Arch Med Sci *7*, 235-241.
Yamashiro, T., Zheng, L., Shitaku, Y., Saito, M., Tsubakimoto, T., Takada, K., Takano-Yamamoto, T., and Thesleff, I. (2007). Wnt10a regulates dentin sialophosphoprotein mRNA expression and possibly links odontoblast differentiation and tooth morphogenesis. Differentiation *75*, 452-462.

Yu, M., Liu, Y., Wang, Y., Wong, S.W., Wu, J., Liu, H., Feng, H., and Han, D. (2020). Epithelial Wnt10a Is Essential for Tooth Root Furcation Morphogenesis. J Dent Res *99*, 311-319.
Zhang, Z., Guo, Q., Tian, H., Lv, P., Zhou, C., and Gao, X. (2014). Effects of WNT10A on proliferation and differentiation of human dental pulp cells. J Endod *40*, 1593-1599.